

## Nuclear Structure of $\text{Ca}^{40,42,44,48}$ from Inelastic Alpha-Particle Scattering\*†

E. P. LIPPINCOTT‡ AND ARON M. BERNSTEIN

*Physics Department Laboratory for Nuclear Science, Massachusetts Institute of Technology,  
Cambridge, Massachusetts*

(Received 8 June 1967)

The  $(\alpha, \alpha')$  reaction has been studied on  $\text{Ca}^{40,42,44,48}$  at 31-MeV incident energy with approximately 90-keV resolution and high statistics. Spin and parity assignments have been made on the basis of systematics and comparison with the distorted-wave Born approximation. Levels of a given spin and parity show remarkably similar angular distributions, even though they vary widely in magnitude. This indicates experimentally that because of the strong absorption of  $\alpha$  particles, the shape of the differential cross section implies the spin and parity of the excited level, and the magnitude indicates the transition strength. The energy levels, spin and parity assignments, and transition strengths found in this experiment are compared with previous experiments and with theoretical results. Two  $4^+$  states, which may be core excitations, have been found in  $\text{Ca}^{40,42,48}$  between 6- and 8.5-MeV excitation energy with an equivalent electromagnetic strength of approximately 0.5 to 3 single-particle units. Three octupole states have been found in  $\text{Ca}^{40,48}$ , six octupole states in  $\text{Ca}^{42,44}$ , a  $5^-$  state in  $\text{Ca}^{40,42,48}$ , and two  $5^-$  states in  $\text{Ca}^{44}$ . The fractionization of the  $3^-$  strength and the rapid and similar drop of the  $3^-$  and  $5^-$  strength in going from  $\text{Ca}^{40}$  to  $\text{Ca}^{44}$  appear to be a challenge to current ideas about the nature of these states.

### I. INTRODUCTION

DURING the past decade there has been considerable theoretical and experimental interest in the structure of the calcium isotopes. In the simple shell-model description of these nuclei,  $\text{Ca}^{40}$  is pictured as a doubly closed shell nucleus and the low-lying positive parity levels of the even- $A$  Ca isotopes are described as  $(f_{7/2})^{A-40}$ . Energy levels and binding energies have been deduced from effective matrix elements of the two-body interaction.<sup>1,2</sup> This scheme has two major difficulties: More levels have been found than are predicted and many electromagnetic transition rates are not explained. To improve this situation, more configurations have been taken into account. To carry out these calculations, interaction matrix elements have either been obtained phenomenologically or, more recently, have been derived from realistic two-nucleon potentials.<sup>3</sup> However, even if the neutrons are allowed to occupy the  $2p_{3/2}$ ,  $2p_{1/2}$ , and  $1f_{5/2}$  shell, in addition to the  $1f_{7/2}$  shell, not all of the low-lying levels can be accounted for. Evidence for rotational sequences of levels have been found<sup>4,5</sup> in  $\text{O}^{16}$  and  $\text{Ca}^{40}$  and collective  $E2$  transition rates have been found in  $\text{O}^{16}$ ,  $\text{O}^{18}$ , and  $\text{Ca}^{42}$  as well as in other presumably spherical nuclei.<sup>6</sup> These facts suggest that

there are deformed states in the doubly closed shell nuclei such as  $\text{O}^{16}$  and  $\text{Ca}^{40}$ .<sup>7,8</sup> Although the precise nature of these deformed states has yet to be determined, experimentally or theoretically, it seems reasonably clear that they are needed to explain the observed spectra and transition rates.

Another interesting class of excitations of the even- $A$  Ca nuclei is the negative-parity levels and, in particular, the  $3^-$  (octupole) states, which are well known from inelastic scattering experiments and are considered to be vibrational states. Recently, they have been given a microscopic description in terms of the particle-hole model.<sup>9</sup> The effects of the residual interactions are to perturb one state downwards in energy and to endow it with a large transition rate (most of the available strength) to the ground state.

Since the octupole mode of excitation is so general, we have attempted to study it in some detail in this experiment.  $\alpha$  particles are useful projectiles for inelastic scattering studies since they are strongly absorbed, which leads to angular distributions which are quite characteristic of the spin and parity of the level excited.<sup>10</sup> Therefore,  $\alpha$  particles are useful not only in strongly exciting collective levels, but also in making spin and parity assignments from the angular distributions.

Because of the intrinsic interest in the states of the even- $A$  Ca isotopes, and because of the merits of inelastic  $\alpha$ -particle scattering experiments, the present experiment was undertaken. The experiment was made possible by the new high-resolution and high-intensity scattering facility at the M.I.T. cyclotron. Some of the

\* Work supported in part by the U. S. Atomic Energy Commission under Contract No. AT(30-1)-2098.

† Based in part on the thesis of E. P. Lippincott, presented in partial fulfillment of the Ph.D. degree requirements.

‡ Present address: Battelle Memorial Institute, Pacific NW Laboratory, Richland, Washington.

<sup>1</sup> I. Talmi and I. Unna, *Ann. Rev. Nucl. Sci.* **10**, 353 (1960).

<sup>2</sup> J. D. McCullen, B. Bayman, and L. Zamick, *Phys. Rev.* **134**, B515 (1964).

<sup>3</sup> T. T. S. Kuo and G. E. Brown, *Nucl. Phys.* **85**, 40 (1965); M. H. Hull, Jr. and C. Shakin, *Phys. Letters* **19**, 506 (1965).

<sup>4</sup> E. B. Carter, G. E. Mitchell, and R. H. Davis, *Phys. Rev.* **133**, B1421 (1964).

<sup>5</sup> R. W. Bauer, A. M. Bernstein, G. Heymann, E. P. Lippincott, and N. S. Wall, *Phys. Letters* **14**, 129 (1965).

<sup>6</sup> For a review of these data see H. E. Gove, Brookhaven National Laboratory Report No. 946, 1965 (unpublished).

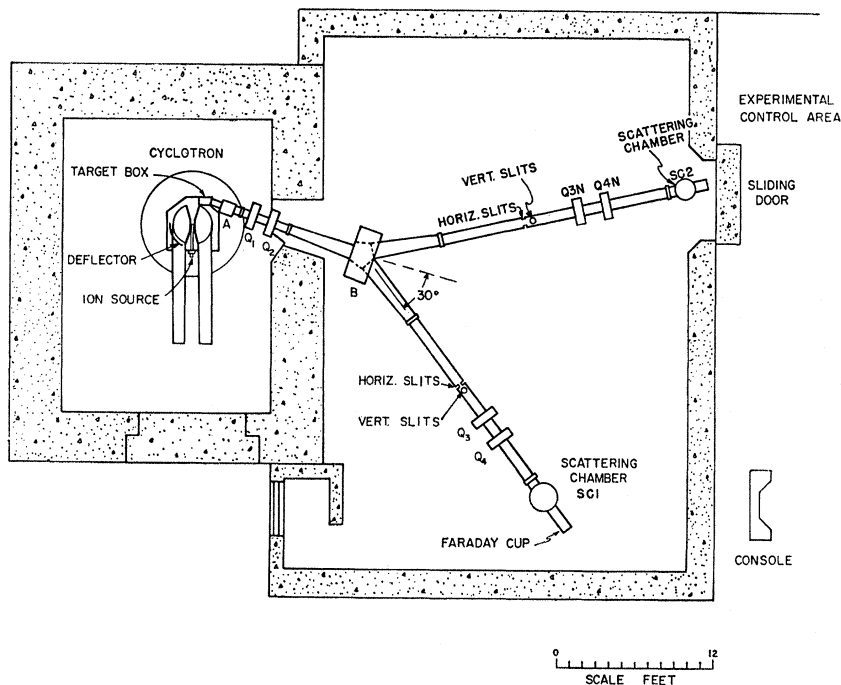
<sup>7</sup> A. Bohr and B. Mottelson (private communication).

<sup>8</sup> G. E. Brown, in *Proceedings of the International Conference on Nuclear Physics, Paris, 1964* (Editions du Centre National de la Recherche Scientifique, Paris, 1965).

<sup>9</sup> For a discussion of the particle-hole model, see G. E. Brown, *Unified Theory of Nuclear Models* (North-Holland Publishing Company, Amsterdam, 1964).

<sup>10</sup> J. S. Blair, *Phys. Rev.* **115**, 928 (1959).

FIG. 1. Layout of the cyclotron beam-handling system. A is an  $8^\circ$  bending magnet, B is a  $30^\circ$  analyzing magnet. Q represents a quadrupole magnet. The scattering chamber used in the present experiment is SC1.



results of the present experiment have been previously reported.<sup>11</sup>

## II. DESCRIPTION OF EXPERIMENT

### A. Equipment

The experiment was carried out using the 31-MeV  $\alpha$ -particle beam of the M.I.T. cyclotron. Figure 1 shows the cyclotron and the apparatus for handling the external beam. The extracted beam from the cyclotron is steered by  $8^\circ$  in bending magnet A and passes through a pair of quadrupole magnets, Q1 and Q2, which, together with the  $30^\circ$  analyzing magnet B, focus the beam at the slits. The installation of A, Q1, and Q2 resulted in an increase in beam intensity by a factor of 10. With typical slit settings of 0.05 in., an energy resolution of  $\approx 70$  keV and a beam intensity of  $\approx 0.3 \mu\text{A}$  can be achieved. The second quadrupole pair, Q3 and Q4, is used to focus the beam on the target in the scattering chamber SC1. Behind the scattering chamber is a Faraday cup which is used for recording beam intensity.

Scattered  $\alpha$  particles were detected by a  $500\text{-}\mu$  silicon surface barrier detector. Pulses from these detectors were handled with conventional electronics (preamplifier, amplifier, biased amplifier, pulse stretcher, and a 1024 channel analyzer). A typical gain setting was  $\approx 15$  keV/channel, and an excitation energy range of  $\approx 12$  MeV was covered.

The targets consisted of foils of metallic calcium approximately  $1 \text{ mg/cm}^2$  thick. Table I gives the isotopic abundances of the target used. The  $\text{Ca}^{40}$  target was made by evaporation of natural calcium metal. The  $\text{Ca}^{44}$  target was prepared by evaporation of separated isotope  $\text{Ca}^{44}\text{CO}_3$  by reducing the carbonate at high temperature during evaporation. The  $\text{Ca}^{42}$  and  $\text{Ca}^{48}$  targets were prepared by the Oak Ridge National Laboratory.

### B. Measurements

Inelastic  $\alpha$  spectra were taken at  $1.8^\circ$  intervals from  $15^\circ$  to  $70^\circ$ . The energy resolution was normally 90–100 keV, and the beam intensity was about  $0.3 \mu\text{A}$ . To get this resolution with the maximum count rate possible, the counters were set to subtend an angle of about  $\frac{3}{4}^\circ$  in the scattering plane.

Angles were measured by a remotely controlled helipot. Relative angles were measured to an accuracy

TABLE I. Ca target composition.<sup>a</sup>

Approx. thickness (in %)	$\text{Ca}^{40}$ 1.1 $\text{mg/cm}^2$ <sup>b</sup>	$\text{Ca}^{42}$ 1.19 $\text{mg/cm}^2$	$\text{Ca}^{44}$ 0.68 $\text{mg/cm}^2$	$\text{Ca}^{48}$ 0.94 $\text{mg/cm}^2$
$\text{Ca}^{40}$	96.92	$4.96 \pm 0.05$	$1.30 \pm 0.05$	$1.93 \pm 0.05$
$\text{Ca}^{42}$	0.64	$93.7 \pm 0.1$	0.04	0.03
$\text{Ca}^{43}$	0.13	$0.19 \pm 0.02$	0.04	<0.01
$\text{Ca}^{44}$	2.13	$1.18 \pm 0.05$	$98.61 \pm 0.05$	0.06
$\text{Ca}^{46}$	0.0032	<0.02	<0.002	<0.01
$\text{Ca}^{48}$	0.179	<0.02	0.01	$97.98 \pm 0.05$

<sup>11</sup> A. M. Bernstein and E. P. Lippincott, Phys. Rev. Letters 17, 321 (1966).

<sup>a</sup> Percentages of calcium isotopes measured before target fabrication.  
<sup>b</sup> Several  $\text{Ca}^{40}$  targets were used in this experiment, all of natural Ca.

of  $0.2^\circ$  and the zero angle was measured to about the same accuracy by scattering on opposite sides of the beam. In some cases, however, the angular error could have been as large as  $0.4^\circ$  because of drifts in the beam over periods of one day.

The beam energy was measured by determining the energy shift of  $C^{12}$  and  $O^{16}$  relative to either  $Au^{197}$  or a Ca isotope. The cyclotron beam energy thus determined varied from 30.5 to 31.5 MeV during the course of the experiment. The uncertainty of each individual measurement was approximately 0.4 MeV, so that it is likely that the primary beam energy varied from run to run but remained constant during the course of each run. Therefore, an energy of  $31.0 \pm 0.5$  MeV was assumed.

### C. Data Analysis

The spectra were plotted by computer and the excited states were visually identified. The cross sections were then determined by a least-squares computer program CYCLOPS based on the routine developed at Los Alamos.<sup>12</sup> Each peak was considered to have a skewed Gaussian shape whose half-width and skew were determined from the elastic scattering peak at that scattering angle. The program required the experimenter to specify the region of interest, the background, the number of peaks to be fitted, and an initial estimate of the peak location and height of each peak. The program then varied the location and height parameters until a best fit to the spectrum was obtained. A given spectrum was generally divided into several regions which were sequentially analyzed by CYCLOPS. The output, consisting of the location, total number of counts, and statistical error for each peak, was punched on cards for input to a second program which correlated the data from all scattering angles. This program was supplied with the laboratory scattering conditions. The  $Q$  values of all groups in the spectrum were calculated taking the relevant kinematics and energy losses in the target into account. For convenience, the results of all angles were regrouped according to  $Q$  value with the restriction that only states that were within  $\pm 30$  keV of each other were considered to belong to the same group. This provided a stringent check on the consistency of the data analysis at each angle, as well as a convenient output.

### D. Cross Sections

To obtain absolute cross sections, the thicknesses of the Ca targets were measured from the energy degradation of  $\alpha$  particles in passing through the foil. The procedure for making absolute cross-section measurements was calibrated by measuring Rutherford scattering from an accurately weighed gold foil. The absolute

cross section obtained for elastic scattering from  $Ca^{40}$  (100 mb/sr at the  $30^\circ$  maximum) is accurate to 10% and agrees to within a few percent of the value obtained independently by Gruhn.<sup>13</sup> The other Ca isotopes were compared to  $Ca^{40}$  at the  $30^\circ$  maximum. The errors for the other isotopes are larger because of uncertainty in target thickness and are estimated to be less than 15% for  $Ca^{42,48}$  and 20% for  $Ca^{44}$ . It should be noted that the elastic cross sections at the  $30^\circ$  and  $45^\circ$  maxima are equal within these errors. A monitor counter, set at a maximum in the elastic scattering cross section, was used to normalize different runs to each other.

There are three main sources of relative errors. First, there is an error because of uncertainty from run to run of the exact alignment of the beam for repeated points. This error over a long series of runs is  $\leq 10\%$ . Second is the statistical error. The remaining error arises from the data analysis from background evaluation and from overlapping peaks caused by either the same element or by contaminants. These latter errors especially affect the weaker states. The large errors at angles where contaminant peaks overlap peaks of interest make data at these angles unobtainable.

In plotting the data, we shall take the normalization error as understood. The data points are plotted without error bars unless either statistical or other errors are greater than 10%. In this paper, we present that part of the data for which spin and parity assignments were made.

### E. $Q$ Values

The  $Q$  values determined in this experiment were made by taking the  $Q$  values of the ground state and several strongly excited states, known from previous work, and then assuming a linear relation between channel number and  $\alpha$ -particle energy. The calibration energies in MeV were  $Ca^{40}$  (3.730, 4.483);  $Ca^{42}$  (1.523, 3.44);  $Ca^{44}$  (1.16, 3.30);  $Ca^{48}$  (3.83, 4.59).<sup>14,15</sup> These calibration energies in the latter three isotopes were checked by comparison with  $Ca^{40}$ . The values of isolated states that could be checked generally agreed to within 10 keV with higher resolution experiments. At higher excitation energies (above 5–6 MeV depending on the nucleus), the level density becomes so great that it is not clear whether the same levels are being compared, so this comparison is not meaningful. It is also more difficult to assign a  $Q$  value to the weaker states and to the states which are not resolved. An uncertainty of  $\pm 30$  keV is assigned as a reasonable average error to the  $Q$  values determined in this experiment.

<sup>13</sup> C. R. Gruhn (private communication); C. R. Gruhn and N. S. Wall, Nucl. Phys. **81**, 161 (1966).

<sup>14</sup> C. M. Braams, Phys. Rev. **101**, 1764 (1956); and thesis, University of Utrecht, 1956 (unpublished).

<sup>15</sup> T. A. Belote, W. E. Dorenbusch, and Ole Hansen, in *Nuclear Spin-Parity Assignments*, edited by N. B. Gove and R. L. Robinson (Academic Press Inc., New York, 1966).

<sup>12</sup> R. H. Moore and R. K. Zeigler, Los Alamos Report No. LA-2367, 1960 (unpublished).

### III. GENERAL RESULTS

#### A. Elastic Scattering and Optical-Model Fits

The elastic scattering cross sections measured in this experiment are shown in Fig. 2. These cross sections have been fitted by an optical-model calculation which computed the scattering from a complex potential well of the form

$$U(r) = -(V + iW)[1 + e^{(r-R)/a}]^{-1}.$$

The code then varies the parameters until a best least-squares fit is obtained.<sup>16</sup> The fits to the data in Fig. 2 are shown as solid lines, and the parameters for the potentials are given in Table II. Optical-model param-

TABLE II. Optical-model parameters for calcium isotopes.

Isotope	$V$	$W$	$R$	$a$
Ca <sup>40</sup>	50.03 MeV	12.39 MeV	5.649 F	0.585 F
Ca <sup>42</sup>	51.27	14.23	5.588	0.625
Ca <sup>44</sup>	53.32	14.62	5.488	0.630
Ca <sup>48</sup>	53.00	14.98	5.624	0.641

eters for  $\alpha$  particles are not determined uniquely by the data,<sup>17</sup> and a variation of parameters with  $V$  similar to the one found by McFadden and Satchler<sup>18</sup> was found. However, the inelastic scattering distorted-wave Born approximation (DWBA) predictions are relatively unaffected by this ambiguity in parameters, and therefore only results based on the parameters in Table II are presented. We note that the optical model does not fit the Ca<sup>40</sup> data for angles greater than 80°.<sup>18</sup>

Elastic  $\alpha$  scattering can indicate the relative sizes of the Ca isotopes. Since these nuclei are quite close in size, it is important to make size-comparison measurements by measuring the angular distribution of the two isotopes relative to each other with high angular precision. Such a measurement has been made and the results are still being analyzed. The present results were not taken with sufficiently high relative angular precision to constitute accurate size comparisons, although the trend of increasing radius with increasing  $A$  can be seen from the shrinking of the diffraction patterns with increasing  $A$ . This effect can also be seen in the inelastic scattering (e.g., Fig. 8).

#### B. Inelastic Scattering and Identification of Spin and Parity

For DWBA calculations,<sup>19</sup> the ingoing and outgoing  $\alpha$ -particle waves were distorted by the optical potential

<sup>16</sup> The optical-model code used was a modification of ABACUS written by E. Auerbach.

<sup>17</sup> R. M. Drisko, G. R. Satchler, and R. H. Bassel, Phys. Letters 5, 347 (1963).

<sup>18</sup> L. McFadden and G. R. Satchler, Nucl. Phys. 84, 177 (1966).

<sup>19</sup> R. H. Bassel, G. R. Satchler, R. M. Drisko, and E. Rost, Phys. Rev. 128, 2693 (1962).

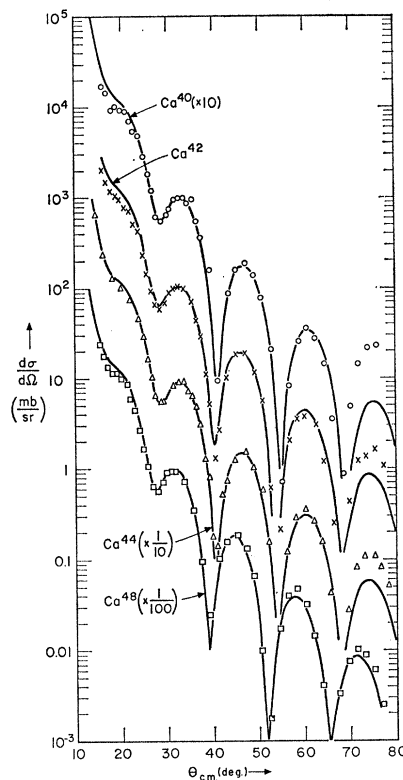


FIG. 2. Elastic scattering cross sections for 31-MeV  $\alpha$  particles from Ca<sup>40,42,44,48</sup>. The solid lines are optical-model fits to the data. The parameters for these fits are given in Table II.

found from the elastic scattering data. The simplest method of calculating angular distributions makes use of the collective model, in which the surface of the nucleus is vibrating about a spherical equilibrium shape according to the formula (to first order)

$$R(\theta', \Phi') = R_0 [1 + \sum_{lm} \alpha_{lm} Y_l^m(\theta', \Phi')].$$

The effect of this oscillation on the optical potential is to introduce nonspherical terms which give rise to inelastic scattering (to vibrational states). This theory has the advantage that the shape of the inelastic scattering cross section is determined completely by the angular momentum transfer and reproduces the Blair phase rules.<sup>10</sup> The only undetermined parameter of the theory is the strength (or magnitude) of the cross section. This is parametrized as  $(\beta_l)^2$ , the root-mean-square deformation of the ground state due to zero point oscillations

$$\beta_l^2 = \langle 0 | \sum_m |\alpha_{lm}|^2 | 0 \rangle.$$

The main features of this theory for strongly absorbed projectiles such as  $\alpha$  particles are that the negative parity states are in phase with the elastic scattering and that positive parity states are out of phase with the elastic scattering cross section. There are also characteristic differences between states of a given parity, but different spin value, in the region of

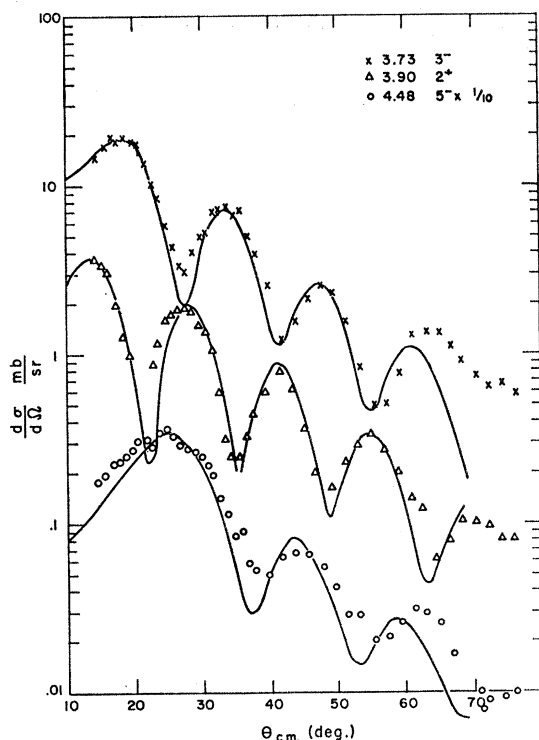


Fig. 3. Inelastic scattering cross sections for the  $3^-$ , 3.73-MeV,  $2^+$ , 3.90-MeV, and  $5^-$ , 4.48-MeV states in  $\text{Ca}^{40}$ .

small momentum transfer. These phase rules are illustrated in Fig. 3 by the scattering to states in  $\text{Ca}^{40}$  which have been previously measured to have the quantum numbers  $2^+$ ,  $3^-$ , and  $5^-$ , respectively. It can be seen that the  $2^+$  and  $3^-$  states are out of phase and a comparison with the elastic scattering data of Fig. 2 shows that the maxima of the  $3^-$  state line up with the elastic scattering maxima. The differences between the  $3^-$  and  $5^-$  states can be seen to be mainly in the vicinity of  $28^\circ$ , where the minimum of the  $3^-$  state is completely missing for the  $5^-$  state. The combination of the high quality of the DWBA fits, as well as the high degree of similarity between states that we infer to be of the same spin and parity, gives us confidence that the spin assignments made in this paper are correct.

For the DWBA calculations we have assumed a collective nuclear model and first-order excitations. However, we also apply this model to states which are not strongly excited. In order to justify this, calculations were performed which indicated that the shapes of the DWBA predictions are not sensitive to the detailed radial shapes of the form factors. This means that although we assume a collective model, we would get essentially the same prediction for any reasonable form factor (for first-order excitations). These calculations show that inelastic  $\alpha$  scattering is a good meter for spin and parity, but not for the detailed radial shape of the wave function. It is important to note that projectiles which are not so strongly absorbed, such as nucleons,

TABLE III.  $2^+$  states.

Nucleus	$E$ (MeV)	$\beta_2$	$G_2^a$	Error in $G_2$ (in %)
$\text{Ca}^{40}$	3.90	0.097	2.7	15
	5.62 <sup>b</sup>	0.046	0.6	25
	7.87 <sup>b</sup>	0.078	1.7	20
	8.10 <sup>b</sup>	0.083	2.0	15
$\text{Ca}^{42}$	8.29 <sup>b</sup>	0.049	0.7	20
	1.52	0.19	10.0	15
	2.42	0.072	1.5	15
$\text{Ca}^{44}$	3.65	0.051	0.75	15
	1.16	0.19	10.0	20
	2.65	0.053	0.81	20
$\text{Ca}^{48}$	4.65	0.059	1.0	25
	3.83	0.13	4.9	15

<sup>a</sup>  $G_2$  is the inferred electromagnetic decay rate in Weisskopf units based on a vibrational nuclear model. (See Sec. III for discussion.) The error in  $G_2$  is based on experimental uncertainties only.

<sup>b</sup> Spin assignment is tentative.

may give much more detailed dynamical information, but are less reliable about inferring spin and parity information.<sup>20</sup>

The significant dynamical quantity measured in  $(\alpha, \alpha')$  reactions is the relative cross sections or  $(\beta_1)^2$ . Assuming

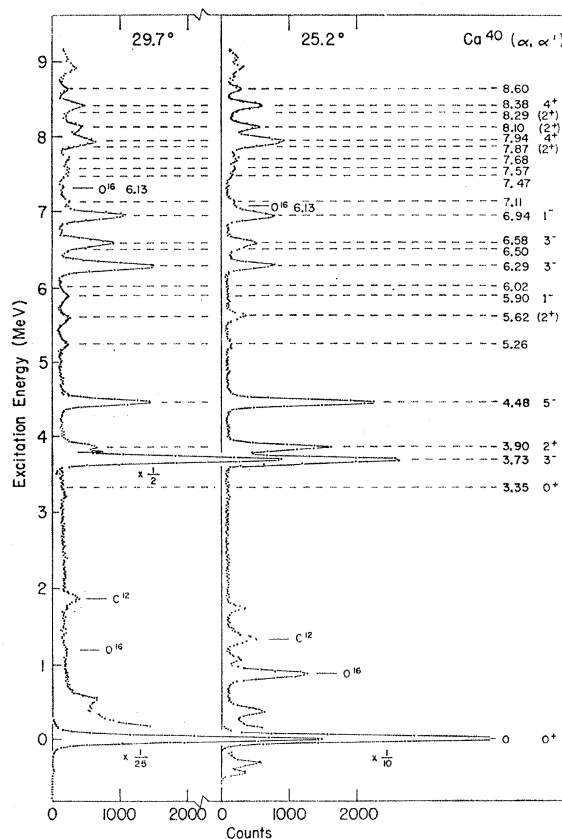


Fig. 4. Spectra of scattered  $\alpha$  particles from  $\text{Ca}^{40}$  at lab angles of  $29.7^\circ$  and  $25.2^\circ$ .

<sup>20</sup> J. S. Blair, in *Proceedings of the International Conference on Nuclear Spectroscopy with Direct Reactions*, edited by F. E. Thow (Argonne National Laboratory, Argonne, Illinois, 1964), Report No. ANL-6848.

TABLE IV.  $4^+$  states.

Nucleus	Excitation energy (MeV)	$\beta_4$	$G_4^a$	Error in $G_4$ (in %)
Ca <sup>40</sup>	7.94	0.094	2.7	15
	8.38	0.083	2.1	15
Ca <sup>42</sup>	2.75	0.067	1.4	15
	4.45	0.077	1.8	20
	5.40 <sup>b</sup>	0.036	0.4	25
	6.51 <sup>b</sup>	0.053	0.9	25
Ca <sup>44</sup>	6.63 <sup>b</sup>	0.048	0.7	25
	2.28	0.046	0.65	20
	5.01	0.067	1.4	20
Ca <sup>48</sup>	6.35	0.072	1.6	25
	6.65	0.065	1.3	25

<sup>a</sup>  $G_4$  is the inferred electromagnetic decay rate in Weisskopf units based on a vibrational nuclear model. (See Sec. III for discussion.) The error in  $G_4$  is based on experimental uncertainties only.

<sup>b</sup> Spin assignment is tentative.

that the neutrons and protons move in phase, as one expects for  $\Delta T=0$  excitations, the value of  $\beta_l$  thus obtained can be used to calculate the electromagnetic transition rate.<sup>21</sup> This procedure is known to underestimate the transition rate and it has been suggested that in comparing  $\beta$  values obtained from inelastic-scattering experiments with those obtained by electromagnetic methods,  $\beta R$  should be compared rather than

$\beta$  itself.<sup>22</sup> Therefore, the inferred electromagnetic transition rate  $G_\lambda$  in Weisskopf units (W.u.) is

$$G_\lambda = \frac{(\lambda+3)^2 (\beta_\lambda Z)^2}{4\pi(2\lambda+1)} \left( \frac{R\alpha}{R_{EM}} \right)^2,$$

where  $R_{EM} \cong 1.2A^{1/3}$  F. In computing values of  $G_\lambda$ , an average value of 1.8 was used for  $(R\alpha/R_{EM})^2$ . Values of  $G_2$  and  $G_4$  with experimental errors are presented in Tables III and IV. The only independent electromagnetic rates that we can compare to the ones inferred from our data are for the lowest  $2^+$  states in Ca<sup>42</sup> and Ca<sup>44</sup> for which the measured values of  $G_2$  of  $8.4 \pm 1.9$ <sup>23</sup> and  $7.7 \pm 1.5$ <sup>24</sup> are in good agreement with the values of  $10 \pm 1.5$  and  $10 \pm 2$  obtained in the present experiment. It should be emphasized that these inferred electromagnetic rates are based on a vibrational nuclear model. It will be interesting to see how well the relative excitation probabilities will compare when more electromagnetic data are available. In particular, it is anticipated that a microscopic theory may predict different relative excitation probabilities for electromagnetic transitions and inelastic  $\alpha$  scattering, particularly for the weaker states.

## IV. RESULTS

### A. Angular Distributions

Inelastic scattering spectra for the isotopes studied are shown in Figs. 4–7. Each spectrum is given at angles of approximately 25° and 30° which favor positive and negative parity states, respectively. The influence of the phase rules on the observed spectra is quite striking. For example, in Fig. 4 we note the difference in intensity of the  $2^+$ , 3.90-MeV state and the  $3^-$ , 3.73-MeV state in Ca<sup>40</sup>. This pair of states also indicates the experimental resolution obtained in this experiment. We note from these spectra that the C<sup>12</sup> and O<sup>16</sup> contaminations are relatively small. Each spectrum can be divided into three distinct regions of excitation energy. Between the ground state and an energy of 5–7 MeV, depending on the nucleus, the states are generally reasonably separated. Above this energy for approximately 2 MeV the observed states are rather dense and sometimes overlapping, and the results are less reliable than for lower excitation energies. Above an energy of 7–9 MeV, no distinct levels are observed. Except for Ca<sup>40</sup>, these energies are several MeV below threshold for nucleon emission. The most likely explanation is that the level density is simply too high for the present resolution and

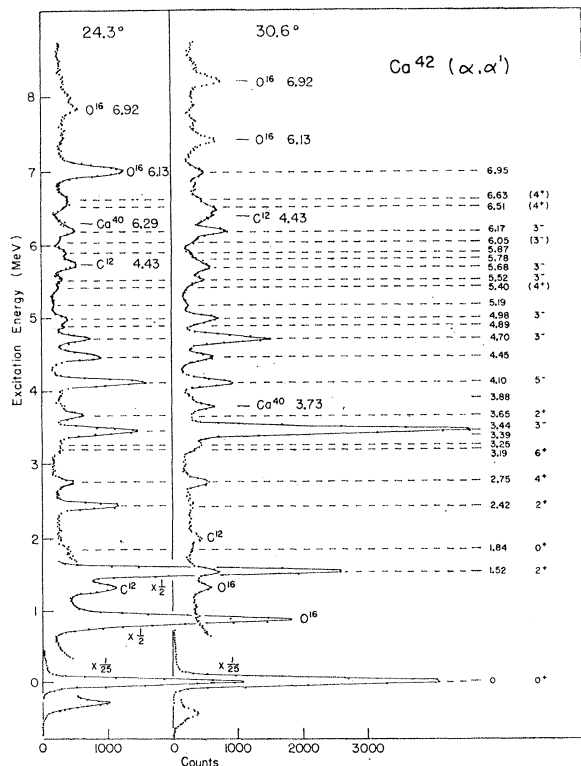


FIG. 5. Spectra of scattered  $\alpha$  particles from Ca<sup>42</sup> at lab angles of 24.3° and 30.6°.

<sup>21</sup> K. Alder, A. Bohr, T. Huus, B. Mottelson, and A. Winther, *Rev. Mod. Phys.* **28**, 432 (1956).

<sup>22</sup> J. S. Blair, in *Proceedings of the International Conference on Nuclear Structure, Kingston, Canada, 1960*, edited by D. A. Bromley and E. W. Vogt (The University of Toronto Press, Toronto, Canada, 1960).

<sup>23</sup> F. R. Metzger and G. K. Tandon, *Phys. Rev.* **148**, 1113 (1966).

<sup>24</sup> D. S. Andrev *et al.*, quoted by P. H. Stelson and L. Grodzins, *Nucl. Data I*, 21 (1965).

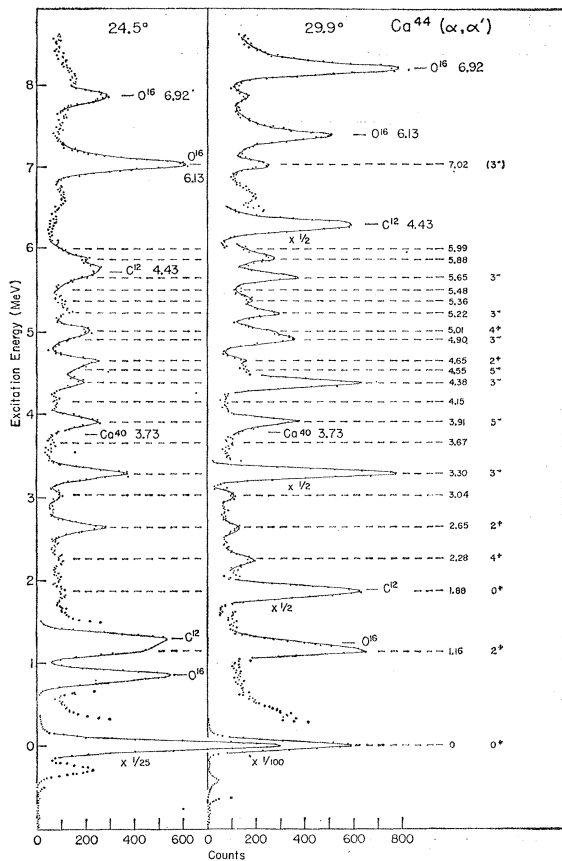


FIG. 6. Spectra of scattered  $\alpha$  particles from  $\text{Ca}^{44}$  at lab angles of  $24.5^\circ$  and  $29.9^\circ$ .

that the states with the large ground-state transition rates are concentrated at lower energies.

In Figs. 8–12, we present the angular distributions of levels for which we were able to make spin assignments. There were also many angular distributions which do not show any definite pattern and are therefore not presented here. Most of these states occur in the region of high-level density and are probably not single levels. We have presented the angular distributions grouped according to their assigned spin values rather than by the target nucleus because of the high degree of similarity of states with a given spin and parity. In these figures, the solid lines are DWBA calculations. Spin and parity assignments which are less certain are shown with an asterisk in Figs. 8 and 9, and these states have parentheses around the spin-parity assignment in the summary graphs (Figs. 15–18). Many of these states will be discussed in Sec. IV B.

Figure 8 presents the data for  $2^+$  states. An interesting feature is that there are three  $2^+$  states each in  $\text{Ca}^{42}$  and  $\text{Ca}^{44}$  and although they are not at the same energies, the lowest states are equally strong, and a factor of 10 stronger than the second and third  $2^+$  states. We note that the DWBA curves do not fit in the vicinity of  $20^\circ$ . The new  $2^+$  assignments from this experiment are  $\text{Ca}^{42}$

(3.65 MeV) and  $\text{Ca}^{44}$  (4.65 MeV) and less definitely  $\text{Ca}^{40}$  (7.87, 8.10, and 8.29 MeV).

Figure 9 presents the data for the  $4^+$  states. In this case, all the assignments except the lowest  $4^+$  states in  $\text{Ca}^{42}$  and  $\text{Ca}^{44}$  have been made on the basis of this experiment. We note that the fits for the  $4^+$  states are not as good as for the  $2^+$  and  $3^-$  states. However, it can be seen that these curves are more similar to each other than they are to the theoretical curves. The differences between the theoretical curves for  $4^+$  and  $5^-$  are shown in Fig. 9(a) for the 8.38-MeV state in  $\text{Ca}^{40}$ . It can be seen that the  $4^+$  gives a better fit to the data than the  $5^-$  curve, particularly, for angles less than  $45^\circ$ . Again, it is worthwhile to note that the distinction between  $4^+$  and  $5^-$  is even clearer when done on an empirical basis.

Figures 10 and 11 give the data for the  $3^-$  states found in this experiment. All the assignments except those for  $\text{Ca}^{40}$  have been made by this experiment. The large number of these states, their similarity, and their relatively large cross sections are striking features of these data and will be discussed later.

Figure 12 gives the data for  $5^-$  states. Again, as was the case for the  $4^+$  states, the theory does not fit quite as well as for the  $2^+$  and  $3^-$  states. However, the fit is sufficiently good to make a spin identification and, again, an empirical comparison shows a high degree of

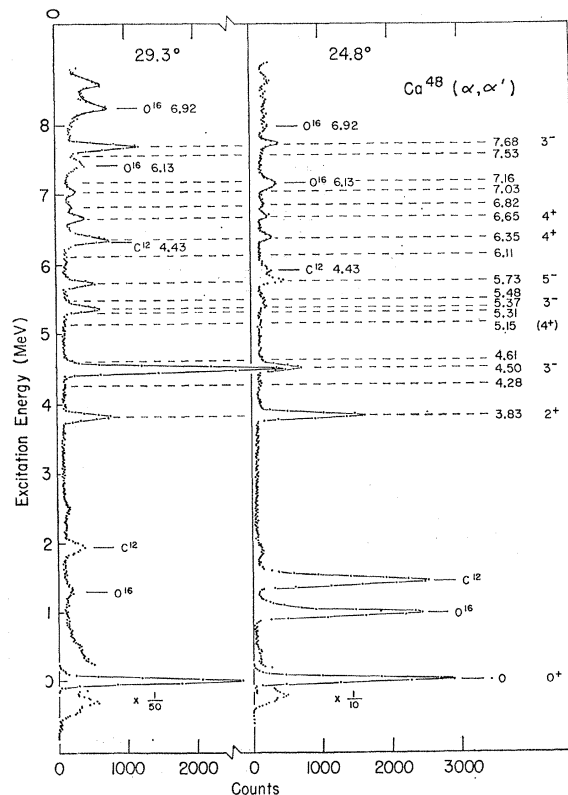


FIG. 7. Spectra of scattered  $\alpha$  particles from  $\text{Ca}^{48}$  at lab angles of  $29.3^\circ$  and  $24.8^\circ$ .

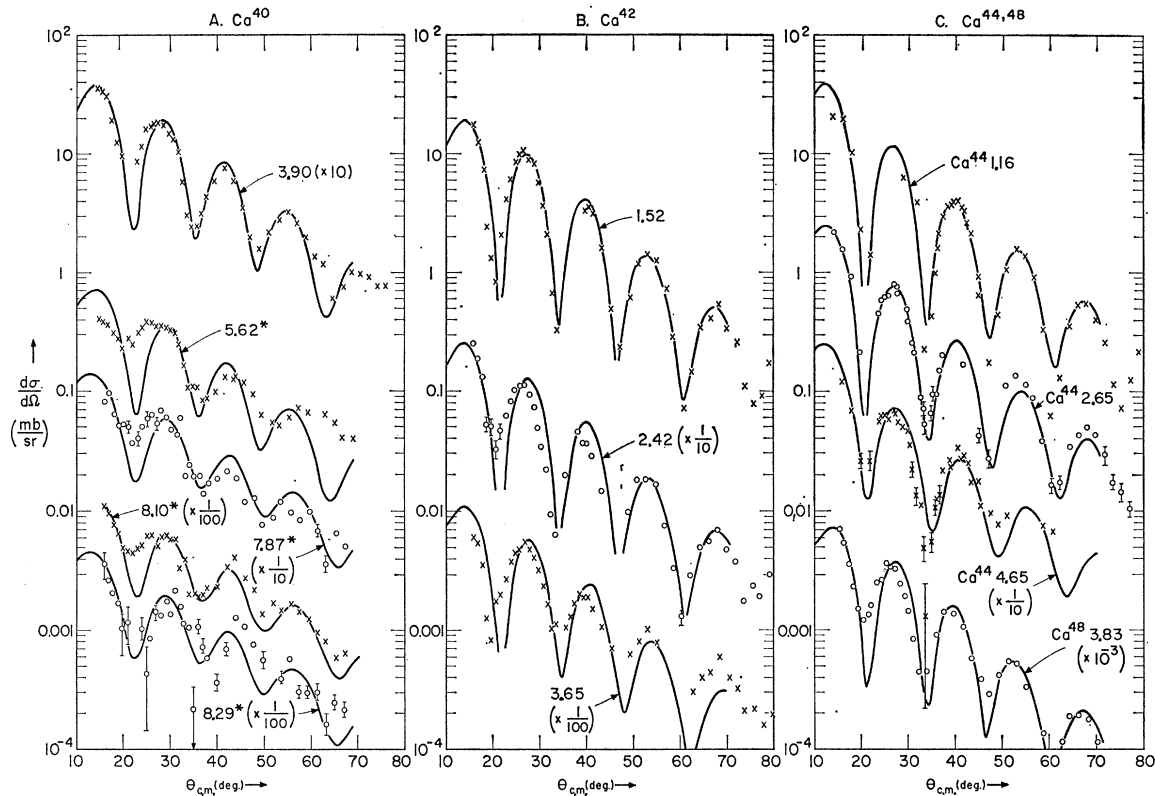


FIG. 8. Cross sections for  $2^+$  states. The solid lines are DWBA calculations. An asterisk indicates states for which the assignments are less certain. (a) gives results for  $\text{Ca}^{40}$ ; (b) for  $\text{Ca}^{42}$ ; and (c) for  $\text{Ca}^{44}$  and  $\text{Ca}^{48}$ .

similarity of the shapes. We note that except in  $\text{Ca}^{40}$  all of the  $5^-$  assignments are new and represent a systematic collective level in each of the nuclei studied.

Two  $1^-$  states have been found in  $\text{Ca}^{40}$  and their angular distributions are shown in Fig. 13. The DWBA fits are done with a collective model with  $L=1$ . The procedure here is not theoretically clear since the  $L=1$  term corresponds to center-of-mass motion. However, it can be shown that the theoretical angular distributions are quite insensitive to the shape of the radial form factor, and only the angular-momentum transfer is important. We therefore use the shape of the theoretical angular distribution, but cannot attach any significance to the deformation parameter obtained by fitting the magnitude of the cross section. It is interesting that the weaker state at 5.90 MeV agrees with the theory much better than the stronger state at 6.94 MeV, particularly in the valleys near  $18^\circ$  and  $32^\circ$ . This appears to be due to the fact that the 6.94-MeV state is really a triplet,<sup>25</sup> which has one  $1^-$  state strongly excited in  $(\alpha, \alpha')$ , and a  $2^+$  state which is excited less strongly. This state will be discussed in detail in the next section.

Figure 13(b) presents the cross sections for three states in  $\text{Ca}^{42}$  which are best fitted by  $L=3$  DWBA

curves. The state at 6.05 MeV has only tentatively been assigned as  $(3^-)$  because of the paucity of data and the relatively large errors. No definite assignment has been made to the 5.19-MeV state because it is weak and data are unavailable at small angles. The 3.25-MeV state fits the  $L=3$  curve best at angles less than  $45^\circ$  but does not have the right envelope at larger angles. This type of discrepancy is characteristic of multiple-step excitations and careful attention has been given to this point in making spin assignments. Multiple excitation for these data is consistent with the results of the  $\text{Ca}^{40}(t, p)$ - $\text{Ca}^{42}$  experiment.<sup>26</sup>

The 5.26-MeV state in  $\text{Ca}^{40}$  which fits the  $L=3$  DWBA theory is presented in Fig. 13(a). This is the weakest state observed in this experiment which might be taken to be  $3^-$ . It is anticipated that the DWBA predictions will deviate from experiment for weak states. To observe this effect, cross-section measurements must be made for states whose spin and parity have been independently measured. For the 5.26-MeV state in  $\text{Ca}^{40}$ , a high-resolution  $(p, p')$  experiment found a close-lying triplet with spin assignments of 0 (1), 2, and 4, respectively.<sup>25</sup> Therefore, spin assignments for states whose cross sections near  $30^\circ$  are less than 0.2

<sup>25</sup> M. A. Grace and A. R. Poletti, Nucl. Phys. **78**, 273 (1966).

<sup>26</sup> S. Hinds and R. Middleton (private communication).

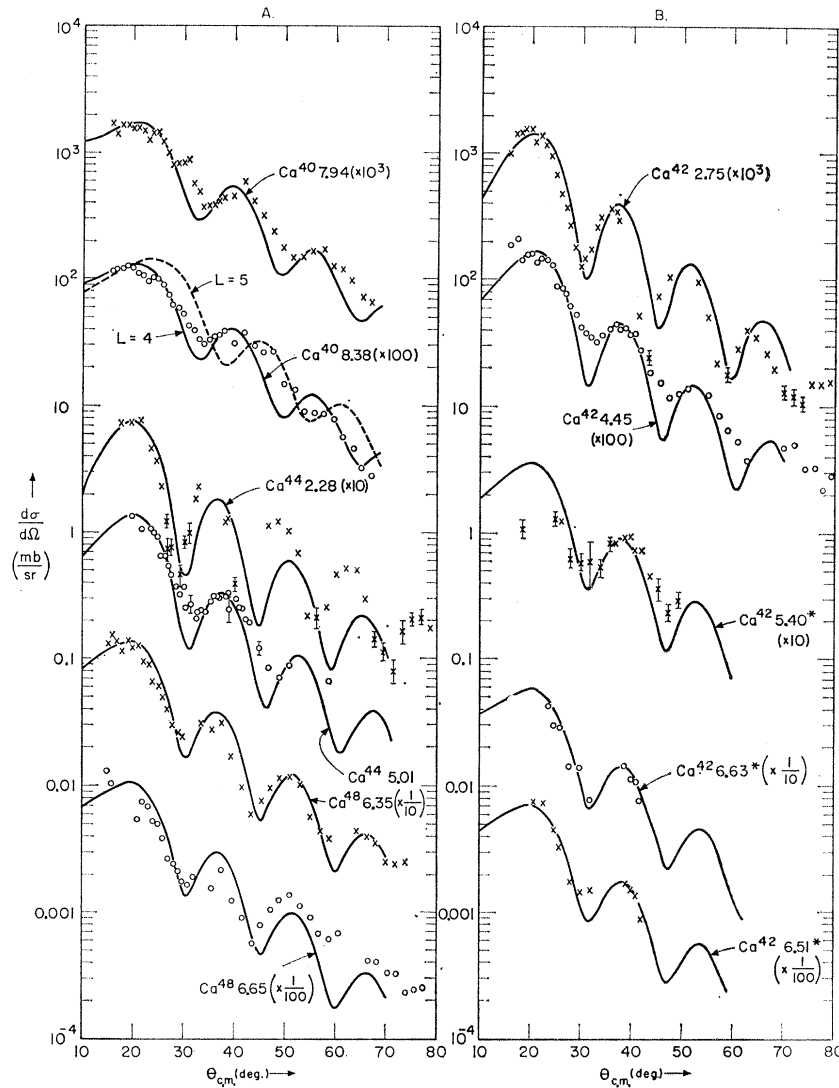


FIG. 9. Cross sections for  $4^+$  states. The solid lines are DWBA calculations. An asterisk indicates states for which the assignments are less certain. (a) shows states in  $Ca^{40,44,48}$ ; (b) shows states in  $Ca^{42}$ .

mb/sr were considered uncertain, if made on the basis of this experiment alone.

In Fig. 14(a) we present the data for the  $0^+$  states of  $Ca^{42}$  and  $Ca^{44}$ . Because of the presence of target impurities and the weakness of these states, the data for smaller angles have large errors. The best data for these states are in the angular region between  $40^\circ$  and  $70^\circ$ . The calculated  $L=0$  DWBA angular distributions do not agree with the data, indicating that these states are not excited by a first-order transition. This agrees with the conclusion of Peterson regarding the excitation of these states with 42-MeV  $\alpha$  particles.<sup>27</sup> The  $0^+$  state of  $Ca^{40}$  was not observed in this experiment because its excitation energy of 3.35 MeV puts it in a place where

it overlaps with the strong  $3^-$  states of  $Ca^{42}$  and  $Ca^{44}$ . In order to get data for this state, a target with less than 0.1%  $Ca^{42}$  and  $Ca^{44}$  would be required. The 4.28-MeV state of  $Ca^{48}$  was identified as  $0^+$  from the  $Ca^{46}(t,p)Ca^{48}$  reaction.<sup>28</sup> Our results for this state were not accurate because of the interference of the  $Ca^{40}$  (3.73 MeV) level. For the  $0^+$  states of  $Ca^{40}$  and  $Ca^{48}$ , the magnitude of the cross section is 2 to 5 times smaller than for the  $0^+$  states in  $Ca^{42}$  and  $Ca^{44}$ .

In Fig. 14 (b), we present data for the known  $6^+$  state<sup>29,30</sup> of  $Ca^{42}$ . In general,  $6^+$  states are weakly excited by  $\alpha$  particles of this energy, and examples of such cross sections are not easy to find. Because of the small

<sup>27</sup> R. J. Peterson, Phys. Rev. **140**, B1479 (1965); Ph.D. thesis, University of Washington, 1966 (unpublished); and to be published. The Ca targets used in this experiment were thin (particularly  $Ca^{48}$ ) and contained large C and O contaminations which allowed proper identification of strong states only.

<sup>28</sup> S. Hinds, J. Bjerregaard, O. Hanson, and O. Nathan, Phys. Letters **21**, 328 (1966).

<sup>29</sup> J. H. Bjerregaard, H. R. Blieden, O. Hansen, G. Sidenius, and G. R. Satchler, Phys. Rev. **136**, B1348 (1964).

<sup>30</sup> P. C. Rogers and G. E. Gordon, Phys. Rev. **129**, 2653 (1963), and references therein.

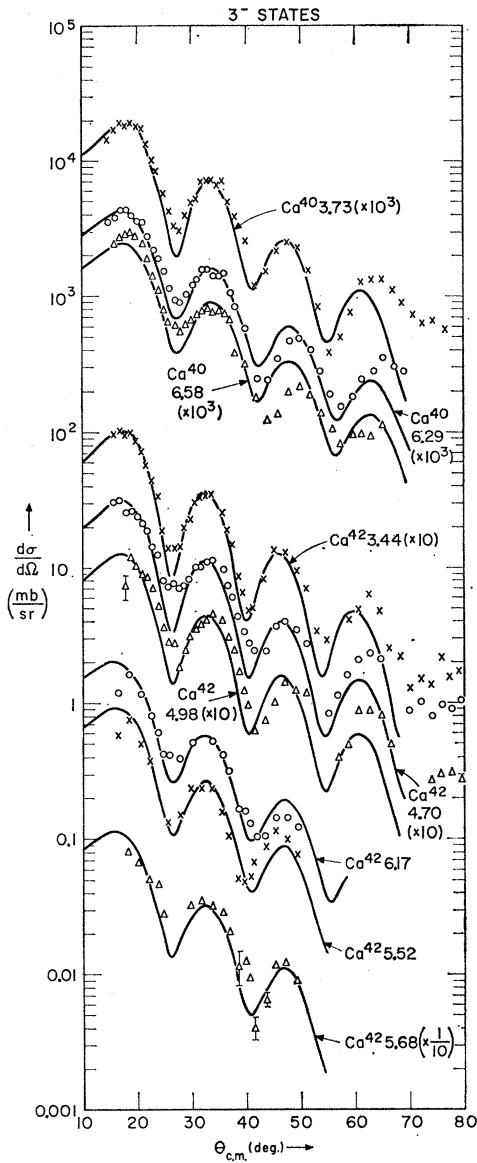


FIG. 10. Cross sections to  $3^-$  states in  $\text{Ca}^{40,42}$ . The solid lines are DWBA calculations.

cross section and the overlap of other nearby levels, errors are large, but the theory for a first-order excitation fits within the accuracy of the experiment.

**B. Specific Nuclei**

In this section, we shall discuss the levels observed in each nucleus and compare these assignments with other experiments and with theory whenever possible. The results of this and other experiments are shown in Figs. 15–18. The systematics of the levels found in this experiment are discussed in the next section,

*Ca<sup>40</sup>—Experimental*

Two  $\text{Ca}^{40}$  spectra are shown in Fig. 4. The levels found in this work and the results of other investigators<sup>25,31</sup> are summarized in Fig. 15. The  $(\alpha, \alpha')$  work reported here is an improvement of the work previously reported<sup>5</sup> in that it has a resolution of 90–100 keV (compared to the previous 120 keV) and about five times the number of counts. The agreement is excellent for the stronger and isolated states. For the weaker and overlapping states, this experiment should be regarded as superseding that work when contradictions exist, and will be discussed below.

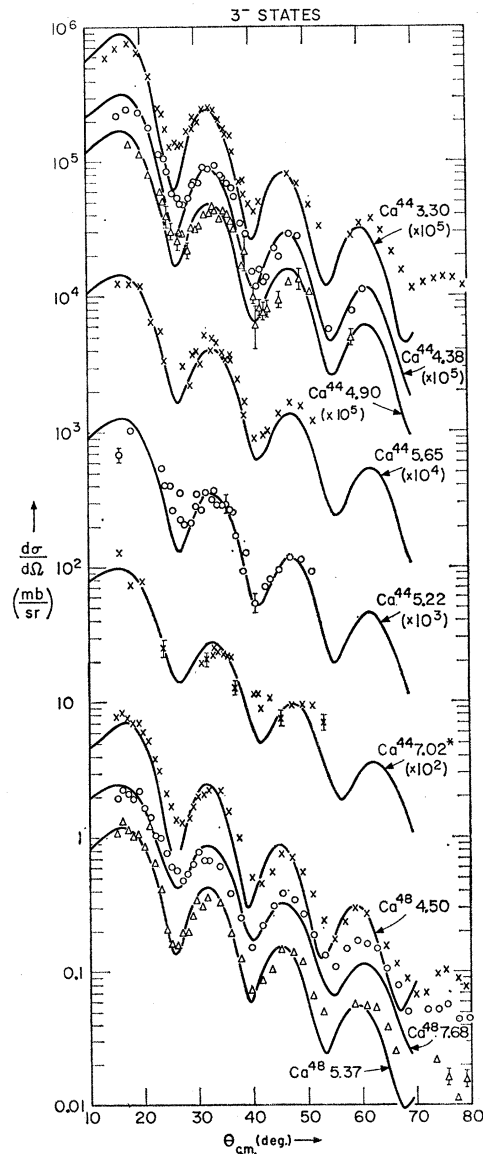


FIG. 11. Cross sections to  $3^-$  states in  $\text{Ca}^{44,48}$ . The solid lines are DWBA calculations.

<sup>31</sup> A. Springer and B. G. Harvey, Phys. Letters 14, 116 (1965).

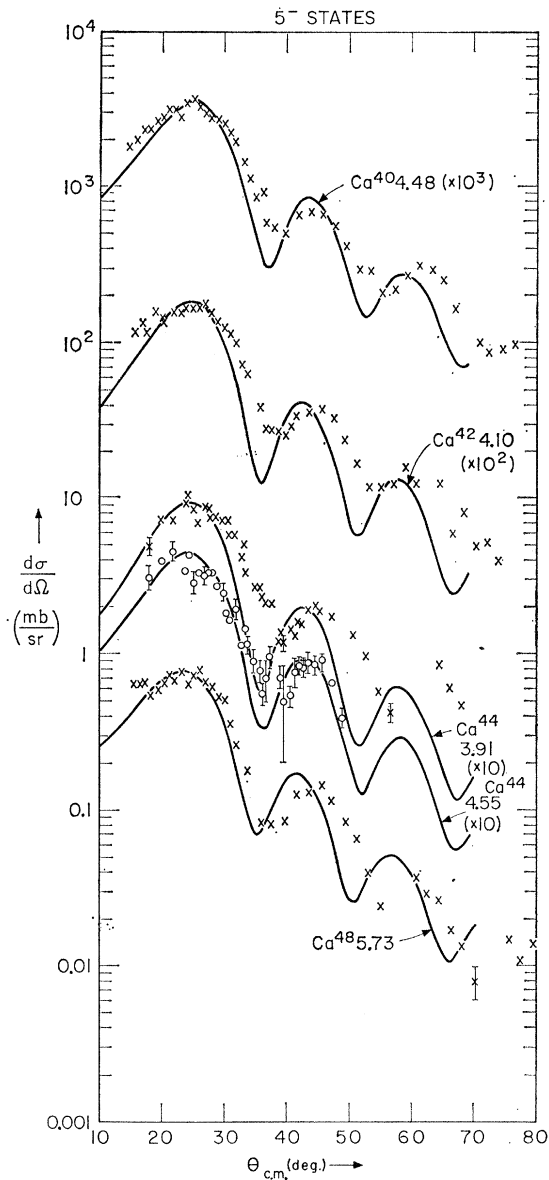


FIG. 12. Cross sections to  $5^-$  states. The solid lines are DWBA calculations.

The structure of  $\text{Ca}^{40}$  has been measured by many other experiments. Two high-resolution experiments have been performed, one at MIT by Braams<sup>14</sup> at 6.5–8.2 MeV with 15-keV resolution, and a second at Aldermaston by Grace and Poletti<sup>25</sup> at 13 MeV with 12-keV resolution. Since the two experiments are in agreement, only the latter is shown in Fig. 15. To measure spins, Grace and Poletti performed a  $(p, p'\gamma)$  experiment with an annular counter set at  $180^\circ$ . In this part of the experiment, their resolution was 45 keV. A  $(p, p')$  experiment has been performed at Colorado at 14 and 17 MeV with 80-keV resolution, and spin assignments were deduced from the angular distribu-

tions with results that are substantially in agreement with the present experiment.<sup>32</sup>

Because of its closed-shell structure,  $\text{Ca}^{40}$  has no states below 3 MeV, and has only four excited states below 5 MeV. The spin and parities of these states are well known. The lowest level at 3.35 MeV is a  $0^+$  state, and was excited weakly, as discussed in Sec. 3 A.

A striking feature of this and previous inelastic-scattering experiments on  $\text{Ca}^{40}$  has been the discovery of three strong  $3^-$  states.<sup>5,31–34</sup> These spin assignments are made on the basis of the angular distribution [Fig. 10(a)] which are remarkably similar in shape, and therefore appear to be quite reliable. In the case of the isolated 6.285-MeV state, Grace and Poletti<sup>25</sup> have verified the spin 3 assignment by an angular-correlation experiment. The systematics of the  $3^-$  states found in this experiment will be discussed more completely in the next section.

Two  $1^-$  states have been identified in  $\text{Ca}^{40}$  [Fig. 13(a)] at 5.90 and 6.94 MeV. The state at 5.90 MeV has been assigned as  $3^-$  by Springer and Harvey<sup>31</sup> using 51-MeV  $\alpha$  particles. Since the difference between  $1^-$  and  $3^-$  can only be seen at small momentum transfers, we believe our assignment to be more accurate. In view of the excellent agreement that we obtain with the  $1^-$  DWBA curve, which is quite different from the  $3^-$  prediction between  $15^\circ$  and  $20^\circ$  at our energy, we conclude that the spin of the 5.90-MeV state is  $1^-$ . This has been confirmed by Grace and Poletti.<sup>25</sup> The state at 6.94 MeV has an angular distribution which is predominantly a  $1^-$ , but which has a smaller  $2^+$  component filling up the minima. This conclusion agrees with Springer and Harvey.<sup>31</sup> In a recent experiment at our cyclotron, the ground-state  $\gamma$  decay of this state has been observed and a  $1^-$  assignment inferred from the angular correlation of the de-excitation  $\gamma$  rays.<sup>35</sup> The Colorado group has observed this level in  $(p, p')$  and  $(\text{He}^3, \text{He}^3')$  reactions and has called this a  $2^+$  level.<sup>32,36</sup> Their assignment agrees with an  $(e, e')$  experiment<sup>33</sup> and a higher energy  $(p, p')$  result.<sup>37</sup> We note that Grace and Poletti<sup>25</sup> have found three levels in this vicinity, so it is quite likely that we are seeing several levels in the various reactions.

The angular distributions for  $2^+$  states in  $\text{Ca}^{40}$  are shown in Fig. 8(a). The state at 3.90 MeV is well known, and the state at 8.10 MeV agrees with the assignment of Springer and Harvey.<sup>31</sup> Tentative assignments of  $2^+$  have been made to states at 5.62, 7.87, and 8.29 MeV. These latter two states occur in a region of

<sup>32</sup> W. S. Gray, R. A. Kenefick, and J. J. Kraushaar, Nucl. Phys **67**, 565 (1965).

<sup>33</sup> D. Blum, P. Barreau, and J. Bellicard, Phys. Letters **4**, 109 (1963).

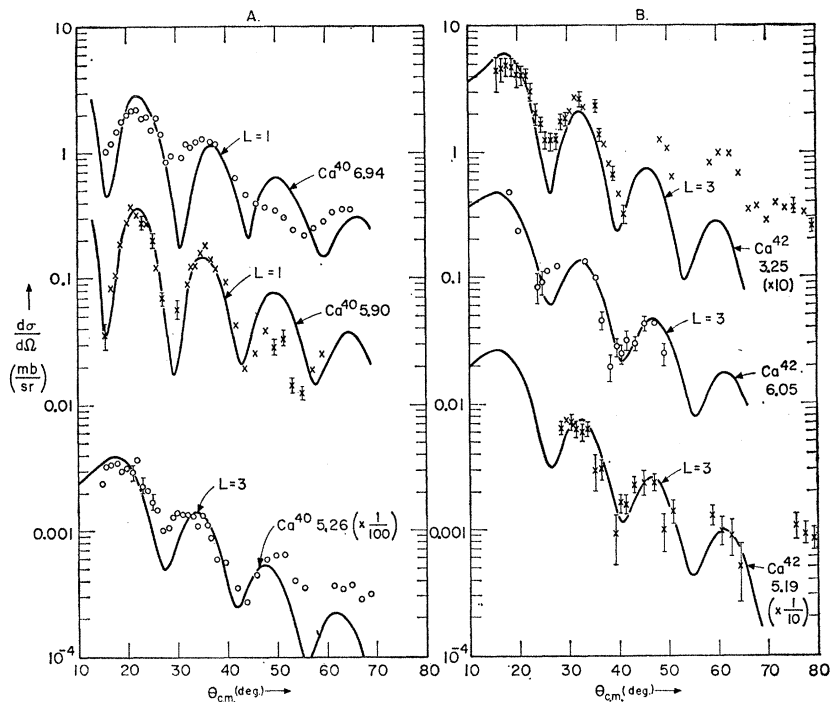
<sup>34</sup> Saudinos *et al.*, Compt. Rend. **252**, 260 (1961).

<sup>35</sup> W. J. Kossler (private communication). W. J. Kossler and K. Nagatani, Bull. Am. Phys. Soc. **11**, 80 (1966).

<sup>36</sup> E. F. Gibson, J. J. Kraushaar, B. W. Ridley, M. E. Rickey, and R. H. Bassel, Phys. Rev. **155**, 1208 (1967).

<sup>37</sup> K. Yagi *et al.*, Phys. Letters **10**, 186 (1964).

FIG. 13. Cross sections to some interesting states in  $\text{Ca}^{40,42}$ . The solid lines are DWBA calculations. For a discussion of these states, see the text.

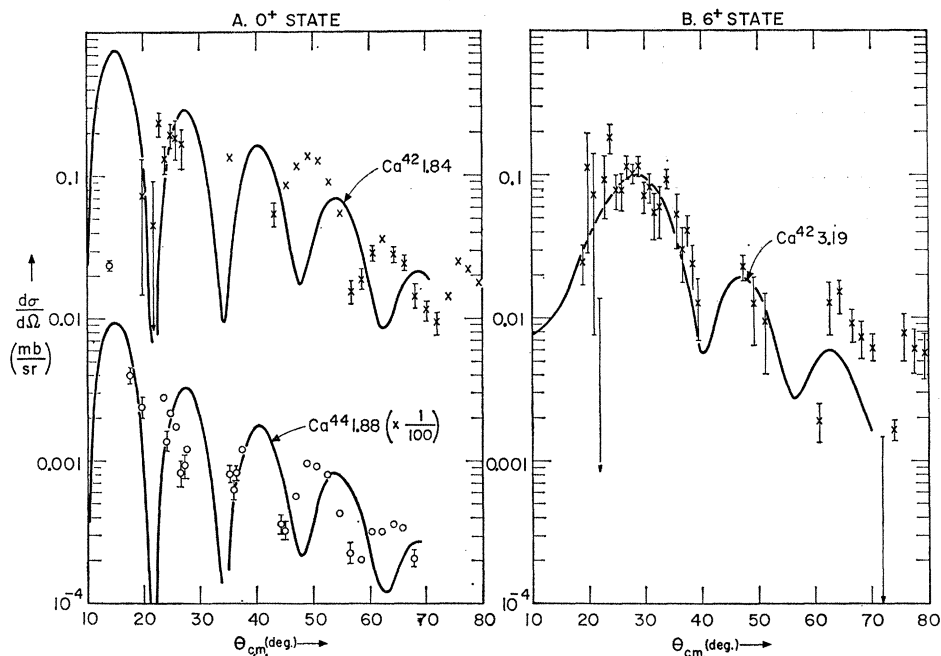


high-level density, and it may be possible that we are seeing more than one state. The 5.62-MeV state was erroneously assigned as  $4^+$  in our previous paper because large errors in the cross section at small angles obscured the dip at  $20^\circ$ . Grace and Poletti observe a spin-2 and -4 doublet in this vicinity,<sup>25</sup> and Erskine

assigns the parity of the spin-4 state as negative.<sup>38</sup> It is consistent, therefore, that we should excite only the natural parity  $2^+$  state, but it is not clear why the dip at  $20^\circ$  is not as deep as the DWBA prediction.

The isolated level at 7.11 MeV<sup>25</sup> was previously observed and thought to have a high spin ( $\geq 6^+$ ).<sup>5</sup> The

FIG. 14. (a) gives the cross sections to  $0^+$  states in  $\text{Ca}^{42,44}$ , (b) gives the cross section to the  $6^+$  state in  $\text{Ca}^{42}$ . The solid lines are DWBA calculations.



<sup>38</sup> John R. Erskine, Phys. Rev. 149, 854 (1966).

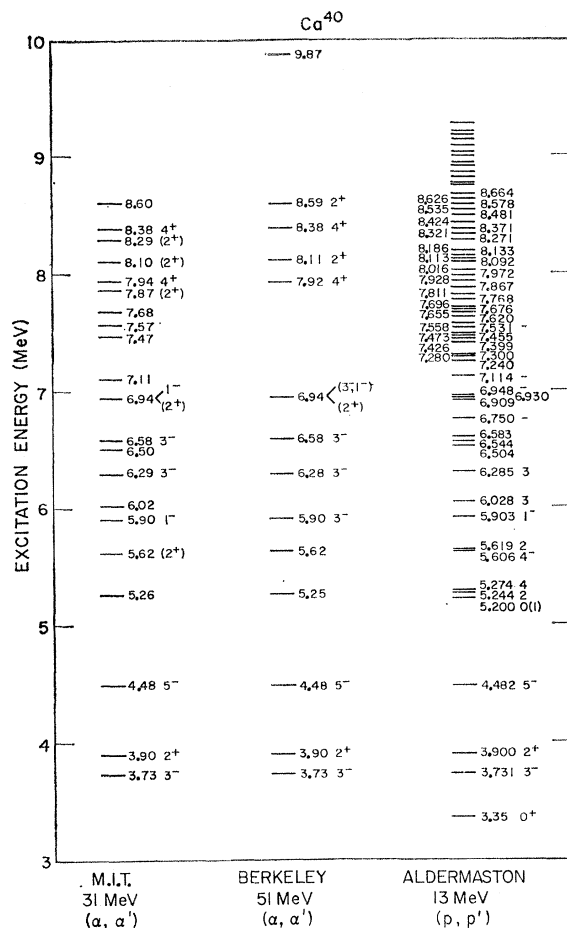


FIG. 15. Energy levels of  $\text{Ca}^{40}$ . In Figs. 15-18 inclusive the column marked M.I.T. 31 MeV ( $\alpha, \alpha'$ ) refers to the present experiment. The other columns are Berkeley, 51 MeV ( $\alpha, \alpha'$ ), Ref. 31; Aldermaston, 13 MeV ( $p, p'$ ), Ref. 25. The parities of the levels above 5 MeV that are indicated in this column were determined by Erskine, Ref. 38.

present data indicate that this state has a rather unusual angular distribution, which does not lend itself to any spin assignment. Therefore, the tentative high spin assignment should be discarded. A  $3^-$  assignment was made for this state by the Colorado group.<sup>36</sup>

Two  $4^+$  assignments have been made to states at 7.94 and 8.38 MeV. Their angular distributions [Fig. 9 (a)] fit the DWBA curves quite well for angles less than  $45^\circ$ , so that these assignments are considered reliable. These assignments agree with Springer and Harvey.<sup>31</sup> The previous assignment of  $5^-$  made for the 8.38-MeV state<sup>5</sup> was incorrect.

The highest state that could be analyzed in the 31-MeV ( $\alpha, \alpha'$ ) spectrum is at 8.60 MeV, but no spin assignment can be made on the basis of the data. It is likely that more than one state is contributing. In the 51-MeV data, this state was seen as a  $2^+$  transition<sup>31</sup> and our data are consistent with that assignment.

$\text{Ca}^{40}$ —Theoretical

In our previous publication on  $\text{Ca}^{40}$ , the possibility of rotational bands was noted.<sup>5</sup> It is interesting to note how this hypothesis has fared under the impact of many new, high-resolution experiments. The possibility of a positive parity rotational band still exists, formed by the 3.35-MeV ( $0^+$ ), 3.90-MeV ( $2^+$ ), and the 5.27-MeV ( $4^+$ ) states. The possible existence of a negative parity rotational band based on the 5.90-MeV ( $1^-$ ) state is uncertain at the present time.

A calculation which assumes the existence of rotational states based on deformed four-particle-four-hole and two-particle-two-hole configurations has been

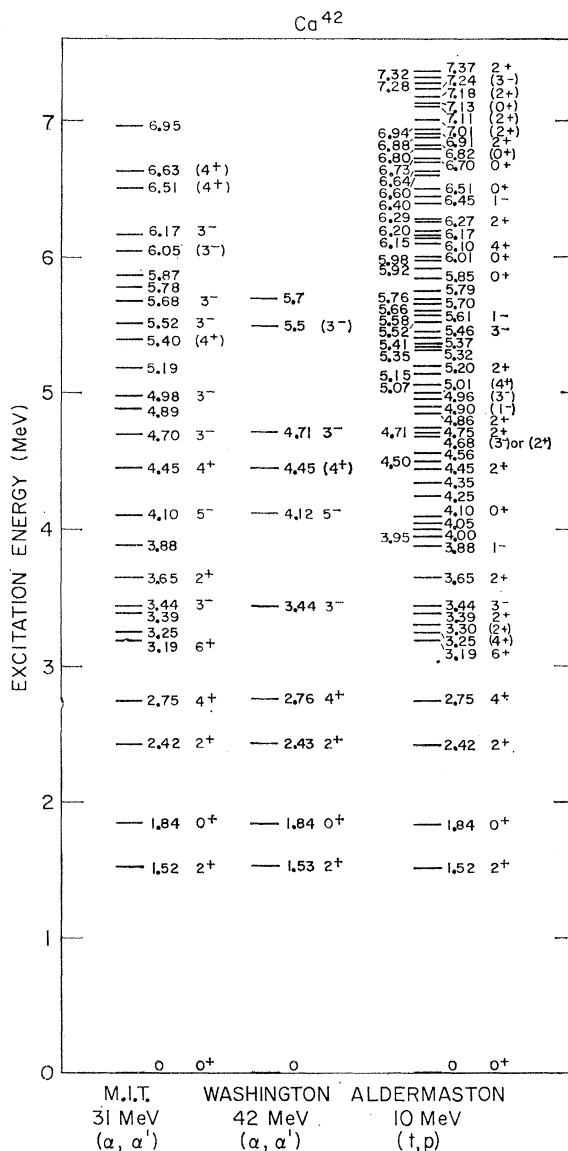


FIG. 16. Energy levels of  $\text{Ca}^{42}$ . Washington, 42 MeV ( $\alpha, \alpha'$ ), Ref. 27; Aldermaston, 10 MeV ( $t, p$ ), Ref. 26.

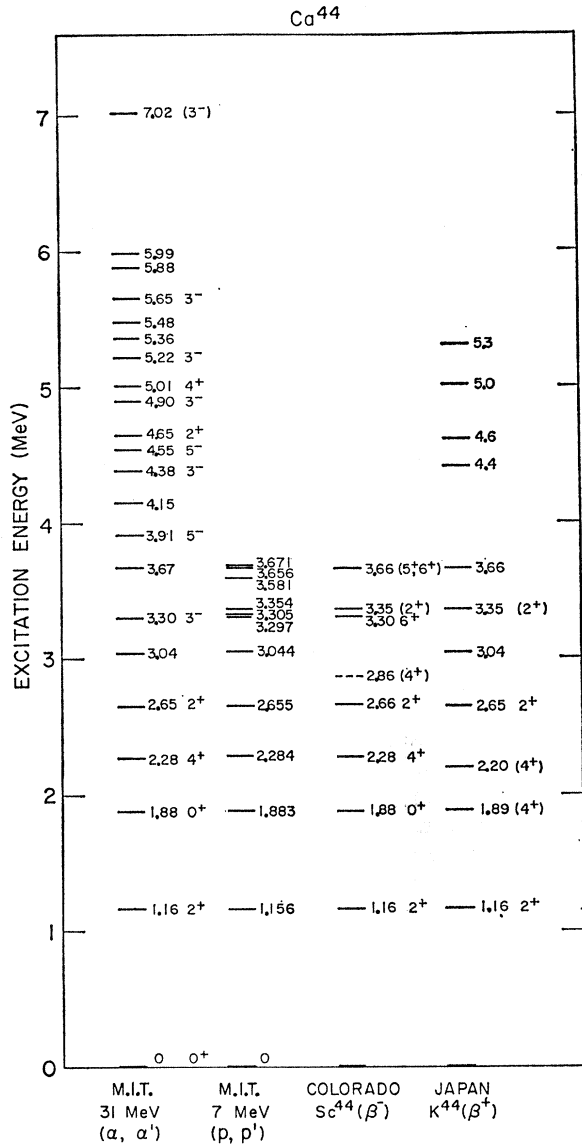


FIG. 17. Energy levels of Ca<sup>44</sup>. M.I.T.; 7 MeV ( $p, p'$ ), Ref. 14; Colorado, Sc<sup>44</sup> ( $\beta^-$ ), Ref. 50; Japan, K<sup>44</sup> ( $\beta^+$ ), Ref. 50.

performed by Gerace and Green.<sup>39</sup> Figure 19 (a) compares the results of their calculation with experiment. The values of the unperturbed energies [which are shown in Fig. 19(a)] are taken to be parameters in such a way as to obtain a good fit to several known states. The effects of diagonalization perturb the upper rotation band so much that the final result does not have the usual sequence for a rotational band. This second rotational band is not well established experimentally although a spin-zero state near 7 MeV has recently been found.<sup>40</sup> The 4<sup>+</sup> level at 7.9 MeV appears to be a candidate for this rotational band. However, the

<sup>39</sup> W. J. Gerace and A. M. Green, Nucl. Phys. A93, 110 (1967).

<sup>40</sup> H. P. Leenhouts, Physica 35, 177 (1967).

angular distribution for this state (Fig. 9) is different and is 10 times as large as for the triplet at 5.26 MeV (Fig. 13) which includes the first rotational 4<sup>+</sup> level. In addition, we note that the  $B(E4)$  values deduced for these states are  $\approx 3$  times larger than are predicted.<sup>41</sup> Therefore, it seems that the 4<sup>+</sup> level at 7.9 MeV has a different origin. (See Sec. V.)

The important predictions of Gerace and Green<sup>39</sup> concern transition rates. These authors predict an  $E2$  transition rate of 0.8 Weisskopf units between the 3.90-MeV state and the ground state, while our experiment indicates a value of 2.3. The validity of this calculation will be tested when more transition rate data are obtained.

The negative parity levels of Ca<sup>40</sup> are shown in Fig. 19(b) along with the one-particle-one-hole calculation of Gillet and Sanderson.<sup>42</sup> Between the 5<sup>-</sup> state at 4.5 MeV and the 4<sup>-</sup>,  $T=1$  level near 7.6 MeV, nine negative parity levels are found, whereas three are predicted. This does not include the 10 unassigned levels in this region, some of which may have negative parity. It

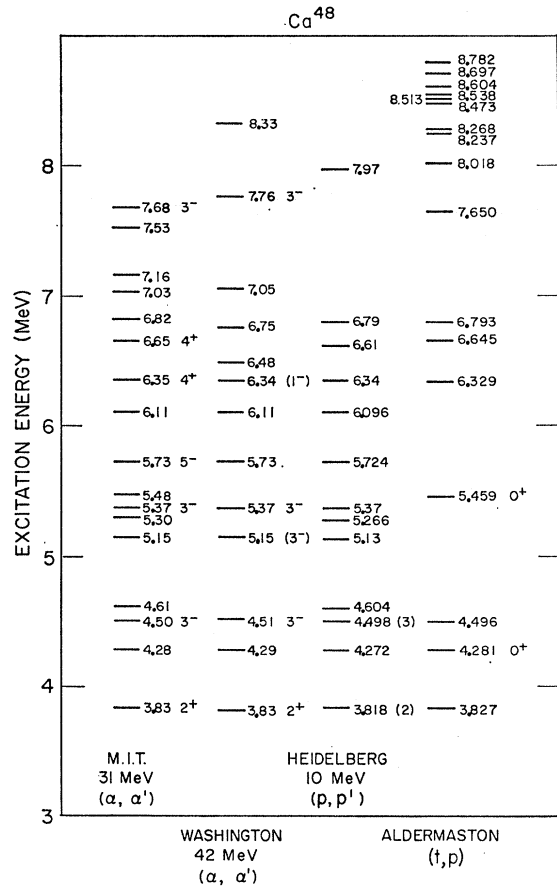


FIG. 18. Energy levels of Ca<sup>48</sup>, Washington, 42 MeV ( $\alpha, \alpha'$ ), Ref. 27; Heidelberg, 10 MeV ( $p, p'$ ), Ref. 54; Aldermaston, Ca<sup>46</sup> ( $l, p$ ) Ca<sup>48</sup>, Ref. 45.

<sup>41</sup> W. Gerace (private communication).

<sup>42</sup> V. Gillet and E. Sanderson, Nucl. Phys. A93, 292 (1967).

appears that more degrees of freedom must be taken into account in order to explain the data.

Transition rates were not calculated by Gillet and Sanderson.<sup>42</sup> However, we note that the energies of the octupole states in this calculation are similar to their previous results.<sup>43</sup> The relative ( $\alpha, \alpha'$ ) cross sections have been calculated for these wave functions<sup>43</sup> by Wall, showing that the three  $3^-$  states between 7 and 8.5 MeV had a total of 10% of the strength of the lowest  $3^-$  state.<sup>44</sup> This must be compared with the experimental strength of 44% of the two observed  $3^-$  states near 6.5 MeV relative to the 3.73-MeV state. Therefore, this calculation,<sup>43</sup> although it properly predicts the absolute strength of the lowest  $3^-$  state for inelastic electron scattering,<sup>45</sup> does not reproduce the strong fractionization of the octupole strength found in inelastic scattering.

The random-phase-approximation (RPA) calculation of Stamp and Mayers<sup>46</sup> for the  $3^-$  states of  $\text{Ca}^{40}$  used a

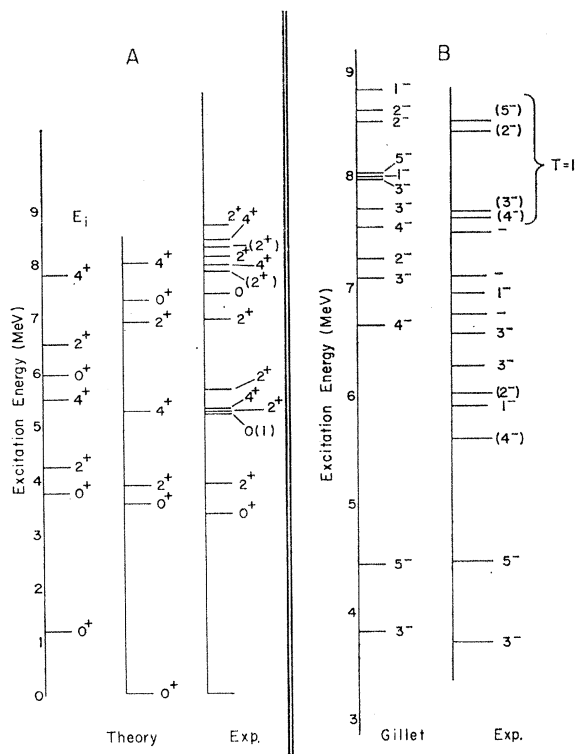


FIG. 19. Experimental theoretical spectra of  $\text{Ca}^{40}$ . (a) shows positive parity states. The theory is due to Gerace and Green, Ref. 39. The column marked  $E_i$  gives their unperturbed energies, and the next column gives their final results. (b) shows negative parity states. The theoretical calculations have been performed by Gillet and Sanderson, Ref. 42. Note the difference in scale between (a) and (b).

<sup>43</sup> V. Gillet and E. A. Sanderson, Nucl. Phys. **54**, 472 (1964).

<sup>44</sup> N. S. Wall, in *Proceedings of the International Conference on Nuclear Spectroscopy with Direct Reactions*, edited by F. E. Thow (Argonne National Laboratory, Argonne, Illinois, 1964), Report No. ANL-6848. N. S. Wall (private communication).

<sup>45</sup> H. P. Jolly, Nucl. Phys. **67**, 209 (1965). V. Gillet and M. A. Melkanoff, Phys. Rev. **133**, B1190 (1964).

<sup>46</sup> A. Stamp and D. F. Mayers, Nucl. Phys. **82**, 296 (1966).

stronger force with the same exchange mixture as that of Gillet and Sanderson,<sup>42</sup> but with a Yukawa interaction and Wood-Saxon wave functions instead of a Gaussian interaction and harmonic oscillator wave functions. The strength of the force is chosen, as in the previous calculation, to put the lowest  $3^-$  state at the experimental energy. Their second and third  $3^-$  states occur at 6.1 and 7.4 MeV with electromagnetic transition rates of 10 and 17% relative to the lowest  $3^-$  state. These positions and strengths are in reasonable agreement with experiment. However, a  $3^-$  state at 10.4 MeV is also predicted with 50% of the ground-state strength. At the present time, there is no evidence for this state.

An RPA calculation which uses matrix elements derived from the Hamada-Johnston potential has been performed by Kuo.<sup>47</sup> The energy of the lowest  $3^-$  state is in agreement with experiment but there is only one  $3^-$  level between 6- and 7-MeV excitation energy. Gerace and Green have added a deformed negative-parity rotational band based on the  $1^-$  state at 5.9 MeV.<sup>41</sup> Their calculation results in octupole states at 3.8, 6.6, and 6.9 MeV with transition rates of approximately 27, 1.9, and 2.7 W.u., respectively. This is in qualitative agreement with the three octupole states found experimentally at 3.73, 6.29, and 6.58 MeV with transition rates of approximately 17, 4.7, and 2.7 W.u., respectively. To test adequately the hypothesis of a negative-parity rotational band, further data are required. We note in this connection that the  $\gamma$ -ray decays of the  $3^-$  states at 6.29 and 6.58 MeV are quite different.<sup>35</sup>

#### $\text{Ca}^{42}$ —Experimental

Figure 5 shows the spectrum of scattered  $\alpha$  particles from  $\text{Ca}^{42}$  at two angles. Many experiments have observed levels<sup>29,30</sup> in  $\text{Ca}^{42}$  in agreement with those of Fig. 16, which compares the results of the present experiment with the high-resolution ( $t, p$ ) experiment<sup>26</sup> and the 42-MeV ( $\alpha, \alpha'$ ) work of Peterson at the University of Washington.<sup>27</sup> The latter experiment was performed on  $\text{Ca}^{42,44,48}$  and on several  $N=28$  nuclei with approximately 150-keV resolution.

An interesting feature of the  $\text{Ca}^{42}$  results is the discovery of six  $3^-$  states (Fig. 10 and Table V). This does not include the tentative  $3^-$  assignment made to the state at 6.05 MeV [Fig. 13(b)]. Furthermore, no assignment has been made to the state at 5.19 MeV [Fig. 13(b)] because it is too weak, even though it appears to fit the  $3^-$  DWBA curve (it would fit a  $1^-$  curve just as well). The agreement between the various experiments concerning the  $3^-$  states is good.

A  $5^-$  state has been discovered at 4.10 MeV (Fig. 12) in agreement with Peterson.<sup>27</sup> The ( $t, p$ ) experiment<sup>26</sup> indicates a  $0^+$  state at 4.10 MeV. In view of the fact that this reaction is very sensitive to  $L=0$  transitions,

<sup>47</sup> T. Kuo (private communication).

and probably fairly insensitive to  $L=5$  transitions to particle-hole states, it appears likely that there is a  $5^-, 0^+$  doublet at 4.10 MeV with the  $0^+$  state not being excited in  $(\alpha, \alpha')$ . A similar situation exists where we have assigned the 6.51-MeV state as  $(4^+)$ , while Hinds and Middleton<sup>26</sup> assign it  $0^+$ . The only discrepancy that may be serious is that we have assigned the 4.45-MeV state as  $4^+$ , while Hinds and Middleton<sup>26</sup> assign it  $2^+$ .

### $Ca^{42}$ —Theoretical

A great deal of theoretical effort has gone into the spectrum of  $Ca^{42}$ . The simplest model of this nucleus is that of two  $f_{7/2}$  neutrons plus an inert  $Ca^{40}$  core. This would give low-lying states of  $0^+, 2^+, 4^+$ , and  $6^+$ . This situation should also hold for  $Ti^{50}$  which would be described as two  $f_{7/2}$  protons plus an inert  $Ca^{48}$  core. Figure 20 presents the spectra of low-lying positive-parity states of  $Ca^{42}$  and  $Ti^{50}$  with some shell-model predictions for  $Ca^{42}$ . For excitation energies up to 3.2 MeV, it is well known that the spectra of  $Ca^{42}$  and  $Ti^{50}$  agree except for the extra  $0^+$  and  $2^+$  states in  $Ca^{42}$  at 1.84 and 2.42 MeV. The calculations of McCullen, Bayman, and Zamick (MBZ)<sup>2</sup> identify the states which are common to  $Ti^{50}$  and  $Ca^{42}$  as belonging to the  $(f_{7/2})^2$

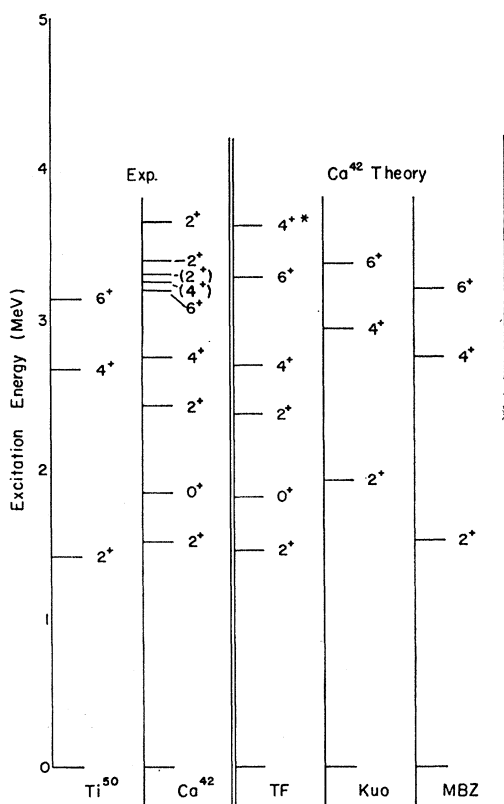


FIG. 20. Experimental spectrum of  $Ca^{42}$  and  $Ti^{50}$  to approximately 3.5-MeV excitation energy with the theoretical predictions of the  $Ca^{42}$  spectrum. The theoretical predictions are MBZ, Ref. 2; Kuo, Ref. 47; and TF, Ref. 49. An asterisk indicates a state not included in the least-squares determination of the effective matrix elements in TF, Ref. 49.

configuration, and from the experimental energies of these states they obtain effective matrix elements for use in other  $f_{7/2}$  shell nuclei (e.g.,  $Ca^{44}$ ).

In order to account for the extra two states, calculations which allow the two active neutrons to occupy the  $f_{7/2}$ ,  $p_{3/2}$ ,  $p_{1/2}$ , and  $f_{5/2}$  levels have been performed by Raz and Soga.<sup>48</sup> This calculation uses empirical values of certain matrix elements in order to get a best fit to the data. They do succeed in getting a  $2^+$  state in the vicinity of 2.42 MeV but not a  $0^+$  state near 1.84 MeV. However, they obtain a  $(p_{3/2})^2, 0^+$  state at 3 MeV while the  $Ca^{40}(t, p)Ca^{42}$  reaction finds a candidate for that state at 5.85 MeV.<sup>26</sup> Therefore, we conclude that this parametrization of the two nucleon interactions is not in accord with experiments.

A recent calculation of Kuo, which allows the neutrons to occupy the four  $pf$  orbitals mentioned above and derives the two-body matrix elements from the Hamada-Johnston potential,<sup>47</sup> is shown in Fig. 20. This calculation gives the  $(p_{3/2})^2, 0^+$  configuration at 5.6 MeV, which is close to the experimental value. It is interesting to note that this calculation fails to account for the second  $0^+$  and  $2^+$  levels. This, plus the large transition rate between the second  $0^+$  and first  $2^+$  levels, supports the hypothesis that the second  $0^+$  level is a deformed hole state based on the  $(d_{3/2})^{-2}(f_{7/2})^4$  configuration. Federman and Talmi<sup>49</sup> have calculated levels in the Ca isotopes between  $Ca^{42}$  and  $Ca^{50}$ , taking the  $f_{7/2}$  and  $p_{3/2}$  shells into account and assuming a deformed state in  $Ca^{42}$  only. The interaction matrix elements were determined empirically by a least-squares fitting procedure. The levels not included in this least-squares fitting procedure are shown with an asterisk in Figs. 20 and 21. Their results are plotted in Fig. 20 and, not surprisingly, the fits below the  $6^+$  level, which were included in the least-squares fitting, are in good agreement with experiment. However, the levels above the  $6^+$  state, which were not included in the fitting, do not agree with the data. (There are three predicted states above the  $6^+$  level which are not shown in Fig. 20.) Above the  $6^+$  state and below the  $(p_{3/2})^2, J=0$  level at 5.85 MeV, only four states are predicted by this theory. The data indicate 10 positive parity levels and 20 unassigned levels in this region. Three of these levels fit into a rotational sequence (whose energies are given below).

Starting with Kuo's wave functions for  $Ca^{42}$ , Gerace and Green<sup>39</sup> have added deformed levels. By adjusting the unperturbed positions of the  $0^+$  levels, they force agreement to the observed energies of the low-lying states. The transition rates are then calculated and are in reasonable agreement with experiment.

The second  $2^+$  state is excited about  $\frac{1}{10}$  as strongly as the lowest  $2^+$  state. Gerace and Green<sup>39</sup> predict a relative  $B(E2)$  value between 4 and 30% of the lowest

<sup>48</sup> B. J. Raz and M. Soga, Phys. Rev. Letters 15, 924 (1965).

<sup>49</sup> P. Federman and I. Talmi, Phys. Letters 22, 469 (1966).



appreciable configuration mixing in these nuclei. This is also indicated by the difference between the  $\text{Cr}^{52}$  and  $\text{Ca}^{44}$  spectrum, which in the  $f_{7/2}$  shell model should be identical. The  $J=4$  configurations have been discussed in the previous section.

Several shell-model calculations which take more configurations into account have been performed. McGrory<sup>52</sup> has used the two-body matrix elements of Kuo, which were derived from the Hamada-Johnston potential, and used them in a basis consisting of an inert  $\text{Ca}^{40}$  core plus four neutrons in the  $f_{7/2}$ ,  $p_{3/2}$ ,  $p_{1/2}$ , and  $f_{5/2}$  configurations. For levels below the  $6^+$  state, the calculation of McGrory predicts the same number of states as MBZ<sup>2</sup>, which suggests that the extra  $0^+$  state at 1.88 MeV and the  $2^+$  state at 2.65 MeV and the  $4^+$  state at 5.01 form a rotational band similar to the situation in  $\text{Ca}^{42}$ . On the other hand, the calculations of Federman and Talmi,<sup>49</sup> which do not include a rotational state in  $\text{Ca}^{44}$ , obtain reasonable fits to the  $0^+$  and  $2^+$  states under discussion. Therefore, the nature of these states will require further investigation.

#### $\text{Ca}^{48}$ —Experimental

The  $\text{Ca}^{48}$  ( $\alpha, \alpha'$ ) spectrum at two angles is shown in Fig. 7. Figure 18 compares these levels with those found by other experiments. Because of the low abundance of

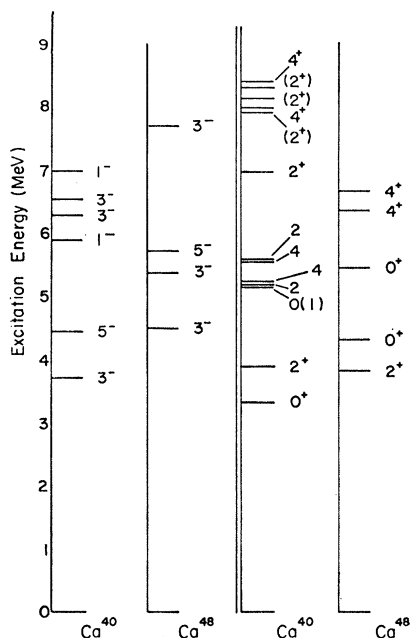


FIG. 22. Comparison of the  $\text{Ca}^{48}$  and  $\text{Ca}^{40}$  spectra. For convenience, this has been separated into negative and positive parity states. For  $\text{Ca}^{40}$  the unnatural parity states and  $T=1$  states have been omitted as comparable states could not have been located in  $\text{Ca}^{48}$  with the present experiments.

<sup>52</sup> J. B. McGrory (private communication); E. C. Halbert, Y. E. Kim, J. B. McGrory, and T. T. S. Kuo, in *Proceedings of the International Conference on Nuclear Physics, Gallatinburg, Tennessee, 1966* (Academic Press Inc., New York, 1967).

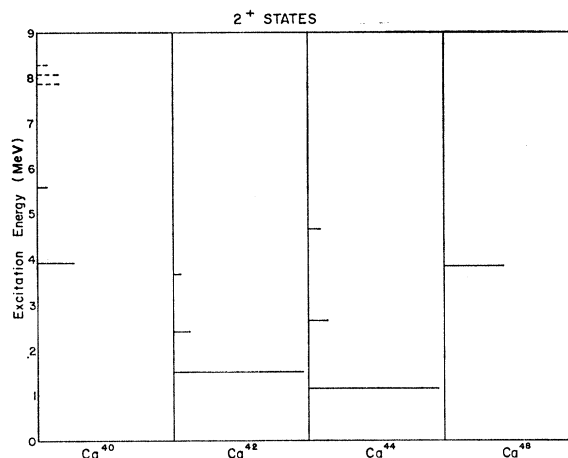


FIG. 23. Systematics of  $2^+$  states. The length of each line is proportional to  $(\beta_2)^2$ . A dashed line indicates that the spin assignment is only tentative.

$\text{Ca}^{48}$ , only a few experiments have been reported on the level structure of this isotope. Recent  $(p, p')$  experiments at Argonne with 11.5-MeV protons<sup>53</sup> and at the Heidelberg tandem<sup>54</sup> with 10-MeV protons have been performed. Since the results of these two  $(p, p')$  experiments are in good agreement, only the Heidelberg results are shown in Fig. 18. The results of the  $\text{Ca}^{46}(t, p)\text{-Ca}^{48}$  reaction performed at Aldermaston are also shown.<sup>28</sup> A  $\text{Ca}^{48}$  ( $\alpha, \alpha'$ ) experiment performed by Peterson<sup>27</sup> had large errors, so that, in our opinion, several of his published spin and parity assignments have little experimental foundation. In Fig. 18, we present Peterson's<sup>27</sup> energy levels with the spin and parity assignments that in our judgment can be made on the basis of his data.

In  $\text{Ca}^{48}$  we have found three  $3^-$  states and a  $5^-$  state. The  $3^-$  assignments are in agreement with Peterson.<sup>27</sup> The spectrum of  $\text{Ca}^{48}$  is compared with  $\text{Ca}^{40}$  in Fig. 22. An interesting difference is that the first excited state of  $\text{Ca}^{48}$  is approximately 0.5 MeV higher than that of  $\text{Ca}^{40}$  and is  $2^+$  instead of  $0^+$ . The first  $0^+$  state of  $\text{Ca}^{48}$  is 0.93 MeV higher than in  $\text{Ca}^{40}$ , the lowest  $3^-$  state is 0.77 MeV higher, and the  $5^-$  state is 1.25 MeV higher. Since shell closure is associated with the energy gap to the excited states, it appears that  $\text{Ca}^{48}$  is a somewhat better closed shell than  $\text{Ca}^{40}$ . We note that in  $\text{Ca}^{40}$  there is a possibility of a  $0^+$ ,  $2^+$ , and  $4^+$  rotation band, where there are no such candidates in  $\text{Ca}^{48}$  at the present. Another interesting feature is the presence of a highly excited  $4^+$  doublet, which is about 1 MeV lower in  $\text{Ca}^{48}$  than in  $\text{Ca}^{40}$ . We are also puzzled by the fact that two  $1^-$  states have been found in  $\text{Ca}^{40}$  but none in  $\text{Ca}^{48}$ . Finally, we note that the lowest  $2^+$  state in  $\text{Ca}^{48}$  was excited 70% more strongly than in  $\text{Ca}^{40}$ .

<sup>53</sup> A. Marinov and J. R. Erskine, *Phys. Rev.* **147**, 826 (1966).

<sup>54</sup> T. Lassen, T. Scholz, and H. J. Unsold, *Phys. Letters* **20**, 516 (1966).

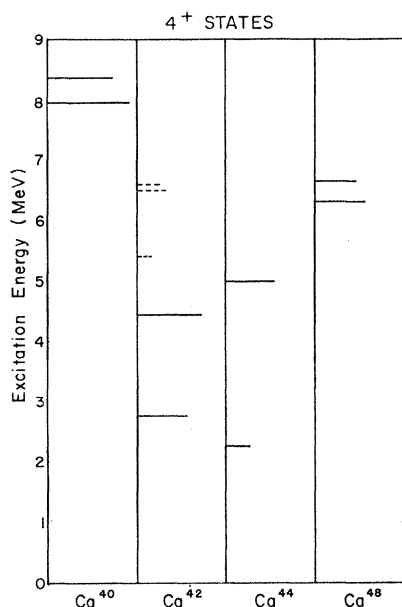


FIG. 24. Systematics of  $4^+$  states. The length of each line is proportional to  $(\beta_4)^2$ .

## V. SYSTEMATICS

### A. Positive Parity States

The energy levels and  $\beta_2$  values found from the DWBA analysis of the  $2^+$  states are listed in Table III and plotted in Fig. 23. The lengths of the lines are proportional to the transition strengths. We note the similarity between  $\text{Ca}^{42}$  and  $\text{Ca}^{44}$ . We also note the paucity of  $2^+$  states in  $\text{Ca}^{48}$  as compared to  $\text{Ca}^{40}$ . The results for  $\text{Ca}^{40,42,44}$  have been compared with theoretical calculations in Sec. IV.

The energy levels and strengths found for  $4^+$  states are given in Table IV, and plotted in Fig. 24. In this case, we have no electromagnetic values to check against. It can be seen that there are two high-lying  $4^+$  states found in  $\text{Ca}^{40}$  and in  $\text{Ca}^{48}$ , with the ones in  $\text{Ca}^{40}$  being stronger and at higher excitation energy. There is a possibility that high-lying states can easily be missed

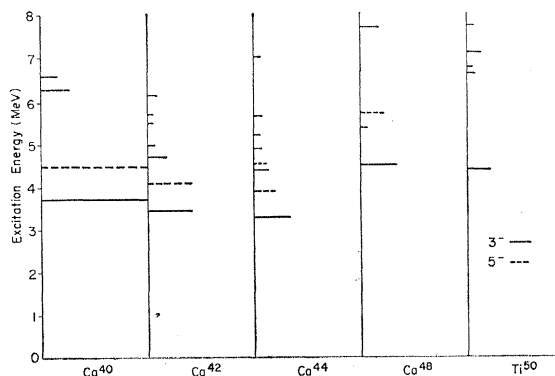


FIG. 25. Systematics of  $3^-$  and  $5^-$  states. The length of the lines are the strengths relative to the lowest  $3^-$  and  $5^-$  state in  $\text{Ca}^{40}$ , respectively.

in more complex nuclei because these states are comparatively weak and would lie in a region of high level density. In  $\text{Ca}^{42}$  we have candidates for  $4^+$  core excited states, while in  $\text{Ca}^{44}$  their absence might not be significant.

There has been theoretical and experimental interest in the occurrence of a systematic  $4^+$  core excitation in nuclei.<sup>55</sup> The position and strength of such an excitation would be related to the  $P_4$  component of the effective two-nucleon interaction. The  $4^+$  levels seen in  $\text{Ca}^{40,48}$  are candidates for this mode of excitation. Since the transition rates are approximately one single-particle unit, these levels are not collective in nature.

### B. Negative Parity States

A significant result of this experiment is the fractionization of the  $3^-$  strength found in the Ca isotopes and the discovery of systematic  $5^-$  states (see Fig. 25). These states have been previously reported.<sup>11</sup> The energies and sums of strengths for the  $3^-$  and  $5^-$  states are presented in Tables V and VI, respectively,<sup>56,57</sup> with their relative strengths  $(\beta^2)$ . The results are presented both in terms of the lowest  $3^-$  state in each nucleus and relative to the lowest  $3^-$  state in  $\text{Ca}^{40}$ . There are two striking points.

First, there are three strong  $3^-$  states in  $\text{Ca}^{40}$  and  $\text{Ca}^{48}$ . At the present time, calculations have been made only for  $\text{Ca}^{40}$  which, as discussed in Sec. IV B, have been qualitatively explained by the inclusion of a negative-parity rotational band.<sup>41</sup>

The second striking point about the octupole strength is the large effect of the valence nucleons. We note that in  $\text{Ca}^{42}$  and  $\text{Ca}^{44}$  we find six  $3^-$  states and in  $\text{Ca}^{48}$  we have found two  $5^-$  states. A natural question is how this fractionization affects the sums of the strengths. The appropriate sums are presented in Table V and in Fig. 26. The fraction of the strengths of the higher excited  $3^-$  states in each nucleus is less in the closed-shell nuclei than in the others. The sum of the  $3^-$  strength drops rapidly in going from  $\text{Ca}^{40}$  to  $\text{Ca}^{44}$ . An intuitive interpretation of either the vibrational or the particle-hole model leads one to believe that the position and strength of particle-hole vibrational levels should be relatively insensitive to shell closures. For the case of the giant dipole state the integrated cross section does not show shell effects, but the width of the giant resonance increases away from shell closures. By analogy, one might expect that the octupole strength would be spread about over a few MeV but that the

<sup>55</sup> B. Mottelson, in *Proceedings of the International Conference on Nuclear Structure, Kingston, Canada, 1960*, edited by D. A. Bromley and E. W. Vogt (The University of Toronto Press, Toronto, Canada, 1960); W. C. Barber, *Ann. Rev. Nucl. Sci.* **12**, 1 (1960).

<sup>56</sup> In Tables V and VI the results for the Ca isotopes are from the present experiment. For  $\text{Ti}^{50}$  we use the data of Ref. 57 for the excitation energies and strengths of the higher excited  $3^-$  states relative to the lowest  $3^-$  state. The strength of the lowest  $3^-$  state in  $\text{Ti}^{50}$  relative to that of  $\text{Ca}^{40}$  has been obtained from Ref. 11.

<sup>57</sup> G. Bruge, J. C. Faivre, H. Farraggi, G. Vallois, A. Bussiere, and P. Roussel, *Phys. Letters* **20**, 293 (1966).

TABLE V. Strength of  $3^-$  and  $5^-$  states.

Nucleus	Excitation energy (MeV)	3 <sup>-</sup> states	
		Relative 3 <sup>-</sup> strength	
		Normalized to lowest 3 <sup>-</sup> state in each nucleus (in %)	Normalized to lowest 3 <sup>-</sup> state in Ca <sup>40</sup> <sup>a</sup> (in %)
Ca <sup>40</sup>	3.73	100	100
	6.29	28	28
	6.58	16	16
Ca <sup>42</sup>	3.44	100	51
	4.70	36	17
	4.98	14	7.1
	5.52	8	4.0
	5.68	11	5.6
Ca <sup>44</sup>	6.17	17	8.7
	3.30	100	34
	4.38	42	14
	4.90	20	6.9
	5.22	16	5.6
Ca <sup>48</sup>	5.65	22	7.6
	7.02	16	5.4
	4.50	100	34
	5.37	18	6.3
Ti <sup>50</sup> <sup>b</sup>	7.68	51	18
	4.42	100	22 <sup>b</sup>
	6.57	36	7.9
	6.72	24	5.3
	7.13	42	9.2
	7.72	18	4.0

Nucleus	Energy	5 <sup>-</sup> states
		Relative 5 <sup>-</sup> strength normalized to 5 <sup>-</sup> state in Ca <sup>40</sup> <sup>c</sup> (in %)
Ca <sup>40</sup>	4.48	100
Ca <sup>42</sup>	4.10	51
Ca <sup>44</sup>	3.91	25
Ca <sup>48</sup>	4.55	12
	5.73	22

<sup>a</sup> The transition strength of the lowest 3<sup>-</sup> state in Ca<sup>40</sup> is 17 Weisskopf units.

<sup>b</sup> Reference 56.

<sup>c</sup> The transition strength of the lowest 5<sup>-</sup> state in Ca<sup>40</sup> is 5.7 Weisskopf units.

observed sum would remain approximately constant. Since this does not appear to be the situation, it is interesting to inquire whether the decrease in the 3<sup>-</sup> and 5<sup>-</sup> strength in adding  $f_{7/2}$  neutrons to Ca<sup>40</sup> can be due to the blocking effect of these neutrons on the particle-hole states. An experimental indication of the importance of blocking can be inferred from the relative behavior of 3<sup>-</sup> and 5<sup>-</sup> states because the  $f_{7/2}$  component of the 5<sup>-</sup> state must be much larger than the  $f_{7/2}$  component of the 3<sup>-</sup> state.<sup>42,46</sup> This is primarily due to

TABLE VI. Sums of strengths of 3<sup>-</sup> and 5<sup>-</sup> states.

Nucleus	Number of 3 <sup>-</sup> states	Sum of	Sum of total	Total 5 <sup>-</sup>
		strengths of 3 <sup>-</sup> states relative to the lowest 3 <sup>-</sup> state (in %)	3 <sup>-</sup> strength in each nucleus relative to the total 3 <sup>-</sup> strength Ca <sup>40</sup> (in %)	strength in each nucleus relative to the Ca <sup>40</sup> 5 <sup>-</sup> state (in %)
Ca <sup>40</sup>	3	44	100	100
Ca <sup>42</sup>	6	86	65	51
Ca <sup>44</sup>	6	116	51	37
Ca <sup>48</sup>	3	69	40	22
Ti <sup>50</sup> <sup>a</sup>	5	120	34	...

<sup>a</sup> Reference 56.

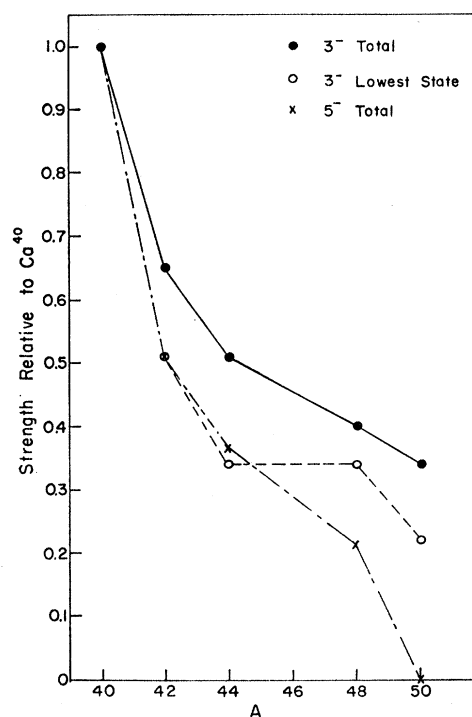


FIG. 26. Variation of 3<sup>-</sup> and 5<sup>-</sup> strengths with atomic mass number. All the points represent Ca isotopes except for A=50 which is Ti. The lines connecting the points are for illustrative purposes only.

the smaller number of particle-hole combinations that can make up the 5<sup>-</sup> state (three for 1  $\hbar\omega$  excitations) than can make up the 3<sup>-</sup> state (nine for 1  $\hbar\omega$  excitations). From the fact that in going from Ca<sup>40</sup> to Ca<sup>44</sup> the sum of the 3<sup>-</sup> strength decreases only somewhat less than sum of the 5<sup>-</sup> strength, it would appear that blocking is not the dominant mechanism. On the other hand, it appears that blocking plays a more significant role in the latter part of the shell because in going from Ca<sup>44</sup> to Ca<sup>48</sup> the energy of the 5<sup>-</sup> state is significantly affected and its strength drops much more rapidly than the sum of the 3<sup>-</sup> strength. At the present time no 5<sup>-</sup> states have been located in the other  $N=28$  nuclei. In addition to blocking, there is also the possibility that the  $f_{7/2}$  shell neutrons can be excited to the next positive-parity levels (e.g.,  $g_{9/2}$ ) to form 3<sup>-</sup> and 5<sup>-</sup> states. The effects of these configurations have not yet been estimated.

It therefore appears that the mechanism for the rapid and similar decrease of the 3<sup>-</sup> and 5<sup>-</sup> strength in going from Ca<sup>40</sup> to Ca<sup>44</sup> is not presently understood. The decrease in strength in going from Ca<sup>44</sup> to Ca<sup>48</sup> is at least partly due to blocking.

## VI. CONCLUSIONS

A high-statistics high-resolution ( $\alpha, \alpha'$ ) experiment has been performed on Ca<sup>40,42,44,48</sup>. The angular distributions to states of a given spin and parity are in excellent agreement with the Blair phase rules and with DWBA calculations which indicate that, because of the strong absorption of  $\alpha$  particles, the shapes of the predicted

differential cross sections are insensitive to the detailed shapes of the radial wave functions. Experimentally, this was demonstrated by the fact that the angular distributions of levels of a given spin and parity are quite similar to each other for angles less than  $60^\circ$ . The angular distributions are sensitive only to the angular-momentum transfer, so that reliable spin and parity assignments can be made. The magnitude of the cross section contains dynamical information about the excited states. By the use of the vibrational model, electromagnetic rates have been deduced and compared with theoretical predictions.

Using the procedures mentioned above, we have made spin and parity assignments to a number of states, and have measured their transition rates.<sup>58</sup> Several  $2^+$

<sup>58</sup> *Note added in proof.* The values of the inferred electromagnetic transition rates in Weisskopf units were derived from a formula based on the vibration of a sharp-edge charge distribution whose radius is taken to be  $1.2 A^{1/3}$ . Because the higher multipolarities strongly weight the surface region, the magnitudes are underestimated. If the measured Fermi-type charge distribution is used, then the transition rates for  $E3$ ,  $E4$ , and  $E5$  transitions would be multiplied by approximately 1.4, 2.1, and 3.3, respectively. These numbers are sensitive to the parameters of the charge distribution and therefore contain an uncertainty which is difficult to estimate. However, there is some evidence that this increase is

states in  $\text{Ca}^{40,42}$  are in reasonable agreement with the results of Gerace and Green.<sup>39</sup> In addition, we have observed a  $4^+$  doublet between 6 and 8.5 MeV in  $\text{Ca}^{40,42,48}$  which appears to be a core excitation. The number of  $3^-$  states and the variation of  $3^-$  and  $5^-$  strength with mass number are not readily explained by our present ideas based on the particle-hole model.

#### ACKNOWLEDGMENTS

It is a pleasure to acknowledge the contribution of N. S. Wall, who designed the external beam system. We would like to thank T. A. Belote, W. J. Kossler, J. Alster, N. S. Wall, and E. F. White for valuable criticisms of the manuscript. The assistance of the cyclotron staff of E. F. White, F. Fay, and J. Byrne was extremely valuable. We would like to thank W. Gerace, T. T. Kuo, A. M. Green, and R. J. Peterson for communicating their results before publication. The programming assistance of T. Provost is gratefully acknowledged.

experimentally required when comparing electromagnetically measured  $E3$  values in light nuclei with those deduced from inelastic scattering experiments. It should be noted that the values of  $\beta_\lambda$  and the relative values of  $G_\lambda$  given in the tables are not altered by this procedure.

### Positron Decay of $\text{Mg}^{22\dagger}$

A. GALLMANN AND G. FRICK

*Institut de Recherches Nucléaires, Strasbourg, France*

AND

E. K. WARBURTON

*Brookhaven National Laboratory, Upton, New York*

and

*Institut de Recherches Nucléaires, Strasbourg, France*

AND

D. E. ALBURGER AND S. HECHTL

*Brookhaven National Laboratory, Upton, New York*

(Received 16 March 1967; revised manuscript received 24 July 1967)

The positron decay of  $\text{Mg}^{22}$  to excited states of  $\text{Na}^{22}$  was investigated using the  $\text{Ne}^{20}(\text{He}^3, n)\text{Mg}^{22}$  reaction to form  $\text{Mg}^{22}$ . The relative cross section for the  $\text{Ne}^{20}(\text{He}^3, n)\text{Mg}^{22}(\beta^+)\text{Na}^{22}$  reaction was measured as a function of  $\text{He}^3$  energy for  $\text{He}^3$  energies between 2.0 and 5.0 MeV. A half-life of  $4.03 \pm 0.05$  sec was obtained for  $\text{Mg}^{22}$ . In addition to the main positron branches to the  $\text{Na}^{22}$  0.657- and 0.583-MeV levels, which were measured to be  $(59 \pm 6)\%$  and  $(36 \pm 6)\%$ , respectively, a branch of  $(5.1 \pm 0.4)\%$  was observed leading to the 1.937-MeV level of  $\text{Na}^{22}$ . The  $\log ft$  for this branch is  $3.55 \pm 0.04$ , which establishes the 1.937-MeV level as  $1^+$ . Upper limits were placed on positron branches to all other excited states of  $\text{Na}^{22}$  below an excitation energy of 3.6 MeV. The  $0.657 \rightarrow 0.583$  transition in  $\text{Na}^{22}$  was found to have an energy of  $73.9 \pm 0.1$  keV. An incidental result was a value of  $472.3 \pm 0.1$  keV for the energy of the  $\gamma$ -ray transition from the isomeric first-excited state of  $\text{Na}^{24}$ .

#### I. INTRODUCTION

THE isotope  $\text{Mg}^{22}$  has a mass excess of  $4.835 \pm 0.020$  MeV with respect to  $\text{Na}^{22}$  and decays to the latter by positron emission.<sup>1-6</sup> Since the nucleus  $\text{Mg}^{22}$  is even-

even, and therefore can be safely assumed to have a spin of  $0^+$ , the positron transition to the  $3^+$  ground

<sup>†</sup> Work at Brookhaven National Laboratory performed under the auspices of the U. S. Atomic Energy Commission.

<sup>1</sup> R. W. Kavanagh, *Bull. Am. Phys. Soc.* **7**, 462 (1962).

<sup>2</sup> P. M. Endt and C. Van der Leun, *Nucl. Phys.* **34**, 1 (1962).

<sup>3</sup> R. E. Benenson and I. J. Taylor, *Bull. Am. Phys. Soc.* **11**, 737 (1966).

<sup>4</sup> J. Cerny, S. W. Cosper, G. W. Butler, R. H. Pehl, F. S. Goulding, D. A. Landis, and C. Détraz, *Phys. Rev. Letters* **16**, 469 (1966).

<sup>5</sup> P. H. Barker, N. Drysdale, and W. R. Phillips, *Proc. Phys. Soc. (London)* **91**, 587 (1967).

<sup>6</sup> The mass excess of  $\text{Mg}^{22}$  used throughout this work is a weighted average of the values given in Refs. 4 and 5 and the two values quoted in footnote 10 of Ref. 4. This average is  $-(347 \pm 20)$  keV on the  $\text{C}^{12}$  scale.